SIMULATING FILAMENTARY STAR FORMATION

Rowan Smith
RAS Norman Lockyer Fellow
JBCA University of Manchester

Simon Glover, Ralf Klessen, Adam Avison, Henrik Beuther, Gary Fuller, Volker Springel

High Mass and Clustered Star Formation: Simulations

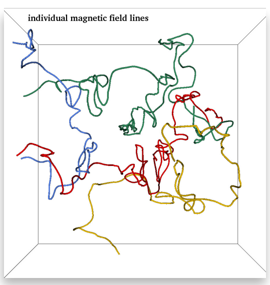

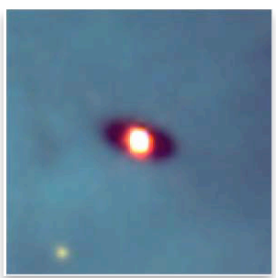

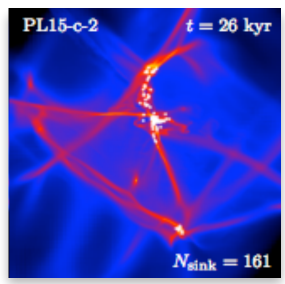

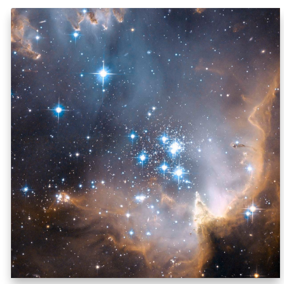

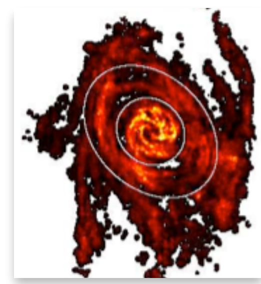

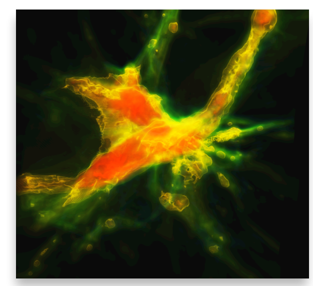

Ralf Klessen

Zentrum für Astronomie der Universität Heidelberg
Institut für Theoretische Astrophysik

agenda

- remarks on star formation theory
  - historic remarks
  - current understanding
- controversies / puzzles
  - column density PDFs: *do we really understand them?*
  - molecular gas: *are we sure we see all H_2 gas?*
  - importance of dynamics: *what sets the IMF?*
  - filaments: *are they universal?*

theoretical remarks

decrease in spatial scale / increase in density


Andromeda (R. Gendler)


NGC 602 in LMC (Hubble)


Proplyd in Orion (Hubble)

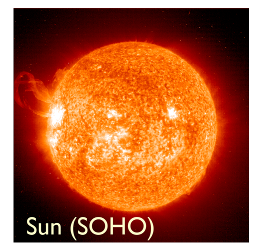
Sun (SOHO)


Earth

- density
  - density of ISM: few particles per cm^3
  - density of molecular cloud: few 100 particles per cm^3
  - density of Sun: 1.4 g/cm^3
- spatial scale
  - size of molecular cloud: few 10s of pc
  - size of young cluster: ~ 1 pc
  - size of Sun: 1.4×10^{10} cm

decrease in spatial scale / increase in density


Andromeda (R. Gendler)


NGC 602 in LMC (Hubble)


Proplyd in Orion (Hubble)

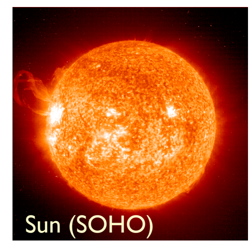
Sun (SOHO)


Earth

- contracting force
  - only force that can do this compression is *GRAVITY*
- opposing forces
  - there are several processes that can oppose gravity
  - *GAS PRESSURE*
  - *TURBULENCE*
  - *MAGNETIC FIELDS*
  - *RADIATION PRESSURE*

Modern star formation theory is based on the complex interplay between *all* these processes.

early theoretical models

- *Jeans (1902):* Interplay between self-gravity and thermal pressure
  - stability of homogeneous spherical density enhancements against gravitational collapse
  - dispersion relation:

$$\omega^2 = c_s^2 k^2 - 4\pi G \rho_0$$

  - instability when $\omega^2 < 0$
  - minimal mass: $M_J = \frac{1}{6}\pi^{-5/2} G^{-3/2} \rho_0^{-1/2} c_s^3 \propto \rho_0^{-1/2} T^{+3/2}$

Sir James Jeans, 1877 - 1946

first approach to turbulence

- *von Weizsäcker (1943, 1951)* and *Chandrasekhar (1951):* concept of ***MICROTURBULENCE***
  - BASIC ASSUMPTION: separation of scales between dynamics and turbulence

    $\ell_{turb} \ll \ell_{dyn}$

  - then turbulent velocity dispersion contributes to effective soundspeed:

$$c_c^2 \mapsto c_c^2 + \sigma_{rms}^2$$

  - → Larger effective Jeans masses → more stability
  - BUT: *(1) turbulence depends on k:* $\sigma_{rms}^2(k)$

    (2) supersonic turbulence → $\sigma_{rms}^2(k) >> c_s^2$ *usually*

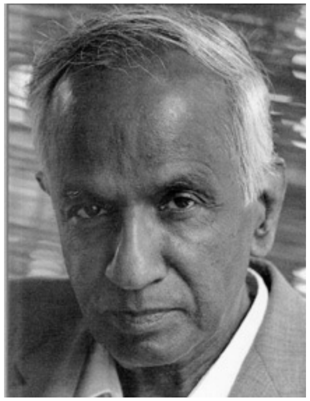

S. Chandrasekhar, 1910 - 1995

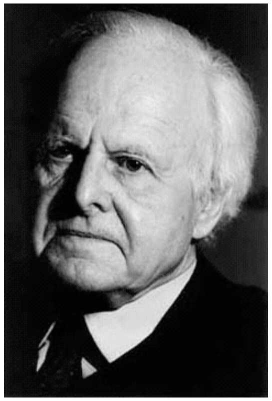

C.F. von Weiszäcker, 1912 - 2007

problems of early dynamical theory

- molecular clouds are *highly Jeans-unstable,* yet, they do *NOT* form stars at high rate and with high efficiency (Zuckerman & Evans 1974 conundrum) (the observed global SFE in molecular clouds is *~5%*)
  → *something prevents large-scale collapse.*
- all throughout the early 1990's, molecular clouds had been thought to be long-lived quasi-equilibrium entities.
- molecular clouds are *magnetized*

magnetic star formation

- *Mestel & Spitzer (1956):* Magnetic fields can prevent collapse*!!!*
  - Critical mass for gravitational collapse in presence of B-field

$$M_{cr} = \frac{5^{3/2}}{48\pi^2} \frac{B^3}{G^{3/2}\rho^2}$$

  - Critical mass-to-flux ratio (Mouschovias & Spitzer 1976)

$$\left[\frac{M}{\Phi}\right]_{cr} = \frac{\zeta}{3\pi}\left[\frac{5}{G}\right]^{1/2}$$

  - Ambipolar diffusion can initiate collapse

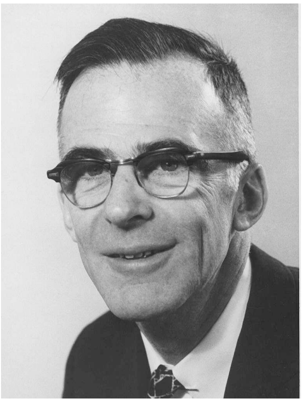

Lyman Spitzer, Jr., 1914 - 1997

“standard theory” of star formation

- BASIC ASSUMPTION: Stars form from magnetically highly subcritical cores
- Ambipolar diffusion slowly increases (M/Φ): $\tau_{AD} \approx 10\tau_{ff}$
- Once $(M/\Phi) > (M/\Phi)_{crit}$: dynamical collapse of SIS
  - Shu (1977) collapse solution
  - $dM/dt = 0.975\ c_s^3/G = \text{const.}$
- Was (in principle) only intended for isolated, low-mass stars

Frank Shu, 1943 -

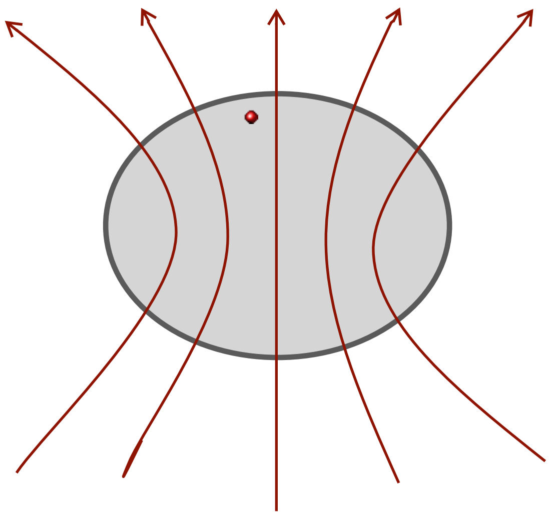

problems of "standard theory"

- Observed B-fields are weak, at most marginally critical (Crutcher 1999, Bourke et al. 2001)
- Magnetic fields cannot prevent decay of turbulence (Mac Low et al. 1998, Stone et al. 1998, Padoan & Nordlund 1999)
- Structure of prestellar cores (e.g. Bacman et al. 2000, Alves et al. 2001)
- Strongly time varying dM/dt (e.g. Hendriksen et al. 1997, André et al. 2000)
- More extended infall motions than predicted by the standard model (Williams & Myers 2000, Myers et al. 2000)
- Most stars form as binaries (e.g. Lada 2006)
- As many prestellar cores as protostellar cores in SF regions (e.g. André et al 2002)
- Molecular cloud clumps are chemically young (Bergin & Langer 1997, Pratap et al 1997, Aikawa et al 2001)
- Stellar age distribution small ($\tau_{ff} << \tau_{AD}$) (Ballesteros-Paredes et al. 1999, Elmegreen 2000, Hartmann 2001)
- Strong theoretical criticism of the SIS as starting condition for gravitational collapse (e.g. Whitworth et al 1996, Nakano 1998, as summarized in Klessen & Mac Low 2004)
- Standard AD-dominated theory is incompatible with observations (Crutcher et al. 2009, 2010ab, Bertram et al. 2011)

(see e.g. Mac Low & Klessen, 2004, Rev. Mod. Phys., 76, 125-194, Klessen & Glover 2014, Saas Fee Lecture, arXiv:1412.5182, 1-191)

properties of turbulence

- laminar flows turn *turbulent* at *high* *Reynolds* numbers

$$Re = \frac{\text{advection}}{\text{dissipation}} = \frac{VL}{\nu}$$

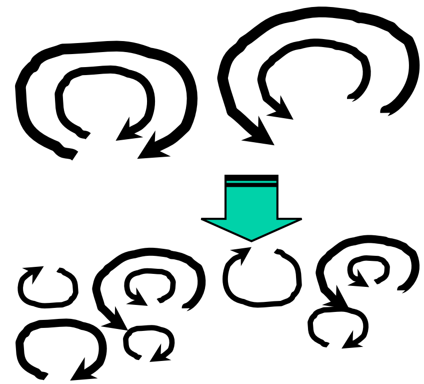

V= typical velocity on scale L, $\nu = \eta/\rho$ = kinematic viscosity,
turbulence for Re > 1000 → typical values in ISM 10^8-10^{10}

- Navier-Stokes equation (transport of momentum)

$$\rho \frac{d\vec{v}}{dt} = \rho\left(\frac{\partial \vec{v}}{\partial t} + (\vec{v}\cdot\vec{\nabla})\vec{v}\right) = -\vec{\nabla}P + \eta\,\vec{\nabla}^2\vec{v} + \left(\frac{\eta}{3} + \zeta\right)\vec{\nabla}(\vec{\nabla}\cdot\vec{v})$$

shear viscosity

bulk viscosity

$$\sigma_{ij} \equiv \eta\left(\frac{\partial v_i}{\partial x_j} + \frac{\partial v_j}{\partial x_i} - \frac{2}{3}\delta_{ij}\frac{\partial v_k}{\partial x_k}\right) + \zeta\delta_{ij}\frac{\partial v_k}{\partial x_k}$$

viscous stress tensor

properties of turbulence

- laminar flows turn *turbulent* at *high* *Reynolds* numbers

$$Re = \frac{\text{advection}}{\text{dissipation}} = \frac{VL}{\nu}$$

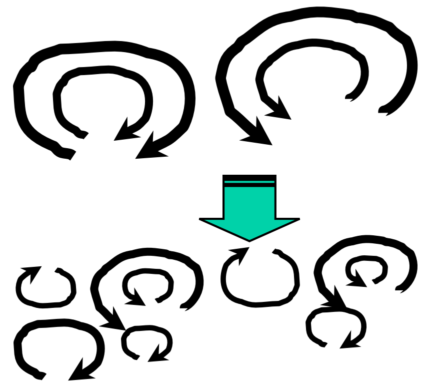

V= typical velocity on scale L, $\nu = \eta/\rho$ = kinematic viscosity,
turbulence for Re > 1000 → typical values in ISM 10^8-10^{10}

- vortex streching --> turbulence is intrinsically anisotropic
(only on large scales you may get
homogeneity & isotropy in a statistical sense;
see Landau & Lifschitz, Chandrasekhar, Taylor, etc.)

(ISM turbulence: shocks & B-field
cause additional inhomogeneity)

turbulent cascade in the ISM

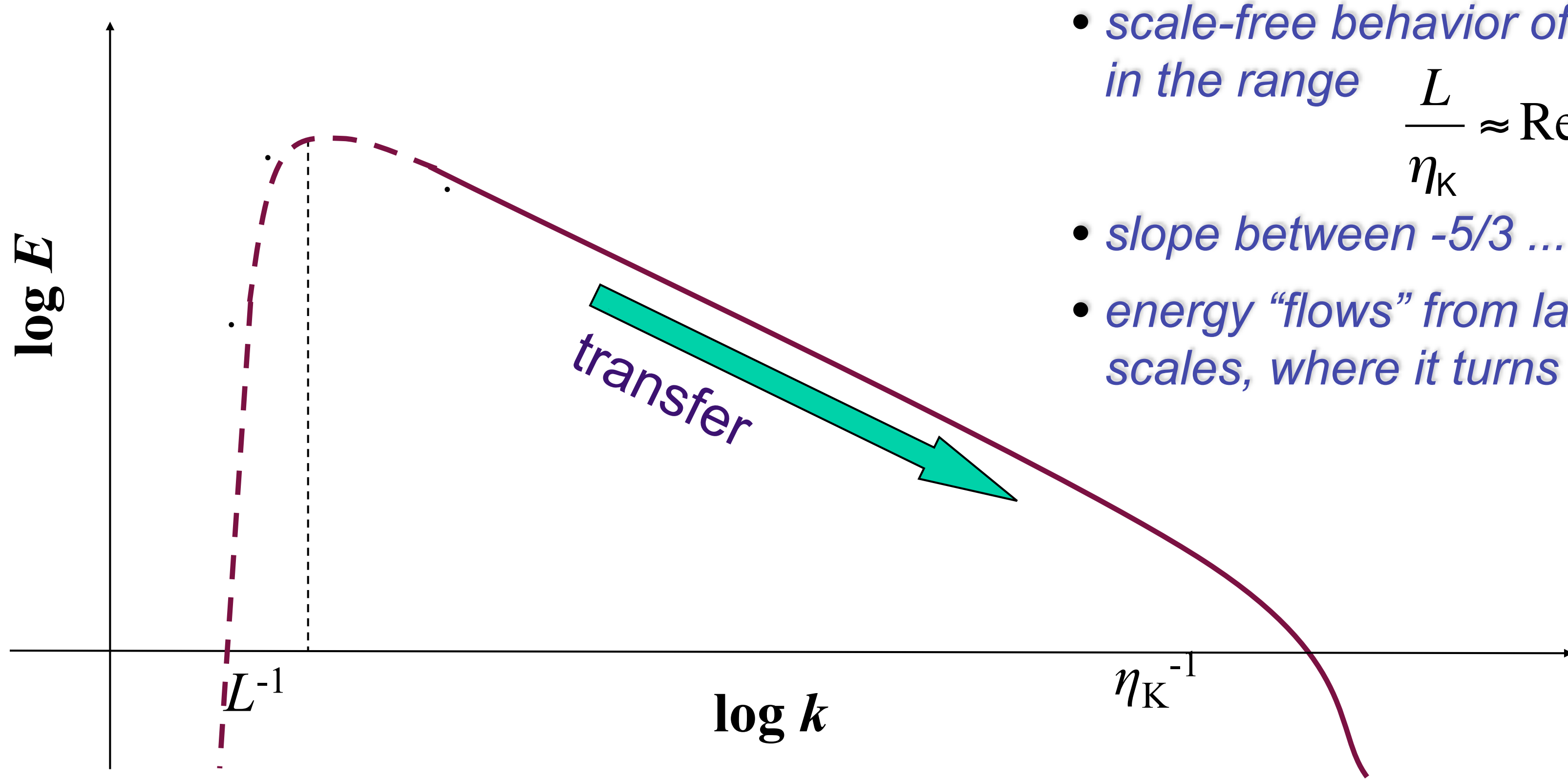

- *scale-free behavior of turbulence in the range* $\frac{L}{\eta_K} \approx \mathrm{Re}^{3/4}$
- *slope between -5/3 ... -2*
- *energy "flows" from large to small scales, where it turns into heat*

energy source & scale *NOT known* (supernovae, winds, spiral density waves?)

dissipation scale not known (ambipolar diffusion, molecular diffusion?)

turbulent cascade in the ISM

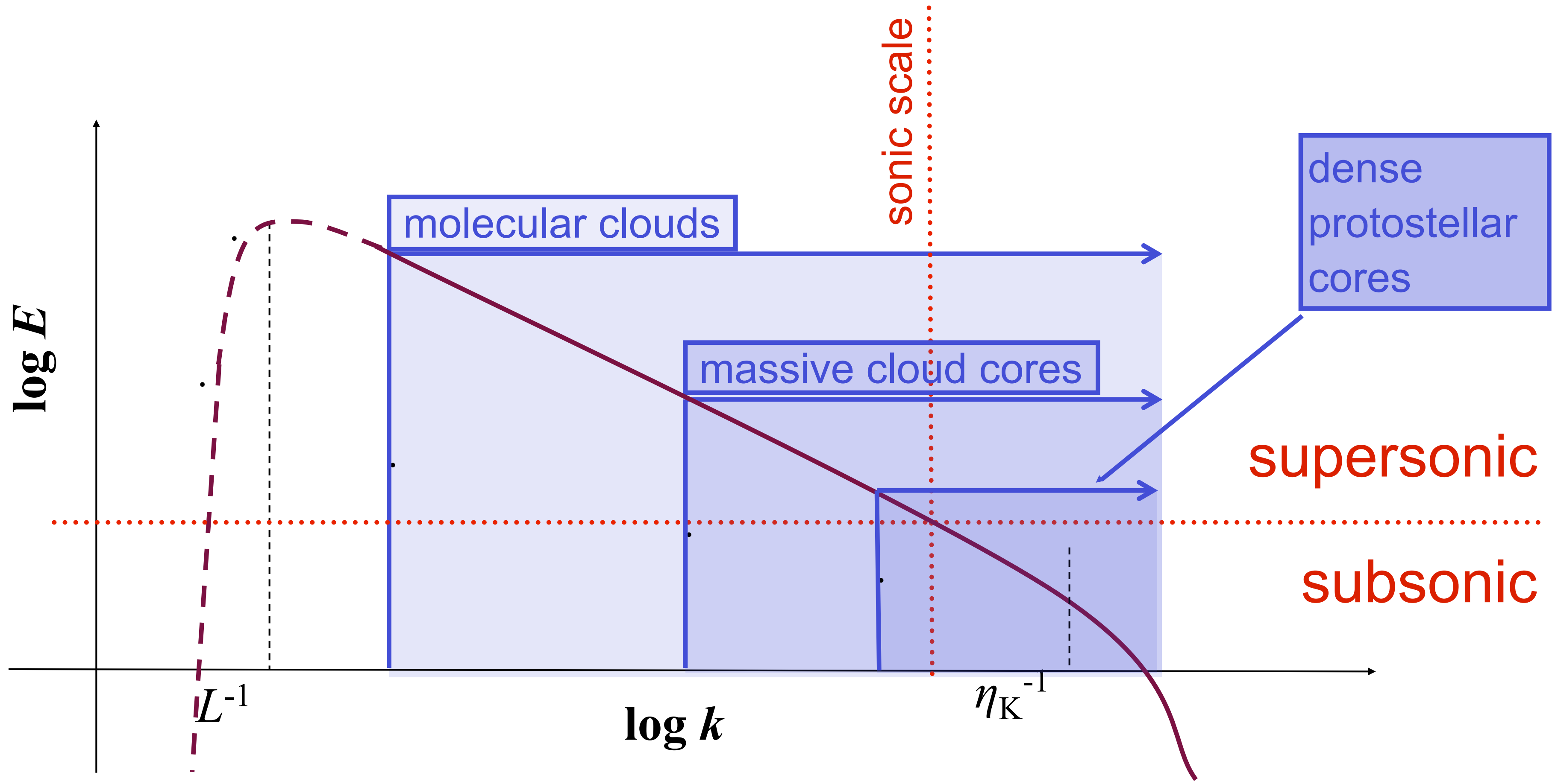

energy source & scale
NOT known
(supernovae, winds,
spiral density waves?)

σ_{rms} << 1 km/s
$M_{rms} \leq 1$
L ≈ 0.1 pc

dissipation scale not known
(ambipolar diffusion,
molecular diffusion?)

gravoturbulent star formation

- BASIC ASSUMPTION:

star formation is controlled by interplay between supersonic turbulence and self-gravity

- turbulence plays a *dual role*:
  - on *large scales* it *provides support*
  - on *small scales* it can *trigger collapse*
- some predictions:
  - dynamical star formation timescale τ_{ff}
  - high binary fraction
  - complex spatial structure of embedded star clusters
  - and many more . . .

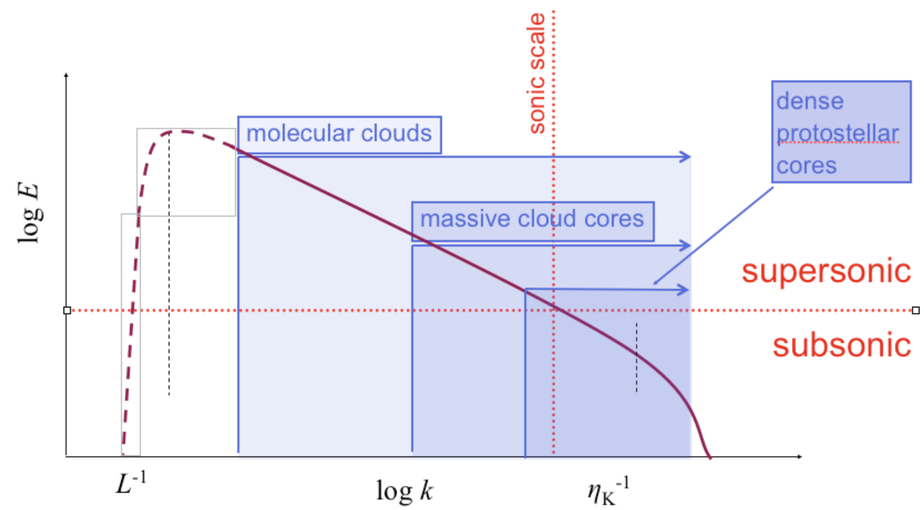

Mac Low & Klessen, 2004, Rev. Mod. Phys., 76, 125-194
McKee & Ostriker, 2007, ARAA, 45, 565
Klessen & Glover 2014, Saas Fee Lecture, arXiv:1412.5182, 1-191

molecular cloud formation

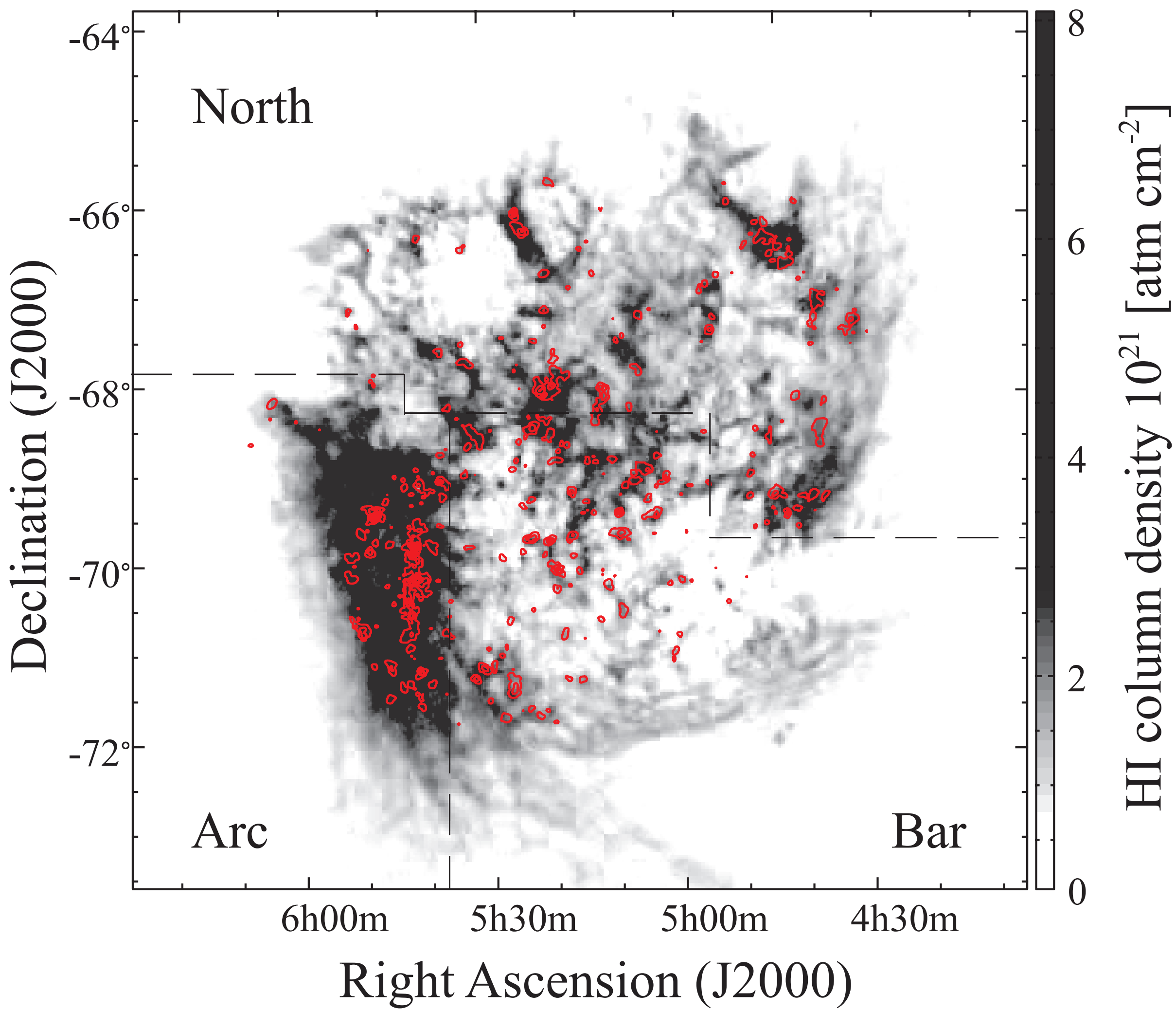

Idea:

Molecular clouds form at *stagnation points* of large-scale convergent flows, mostly triggered by global (or external) perturbations. Their internal turbulence is driven by accretion, i.e. by the process of cloud formation

- molecular clouds grow in mass
- this is inferred by looking at molecular clouds in different evolutionary phases in the LMC (Fukui et al. 2008, 2009)

Fukui et al. (2009)

zooming in ...

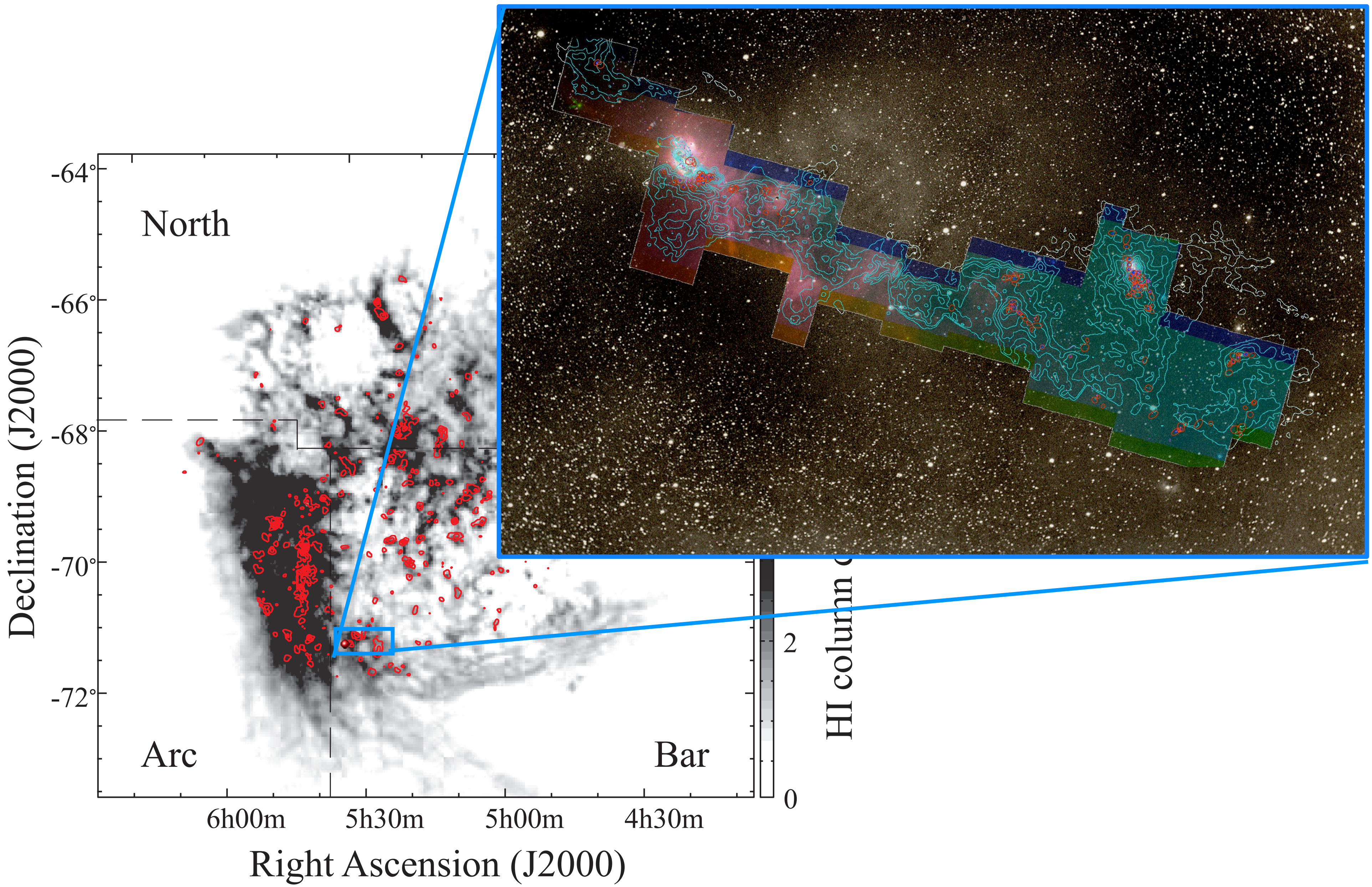

-64°
-66°
-68°
-70°
-72°
North
Arc
Bar
Declination (J2000)
6h00m
5h30m
5h00m
4h30m
Right Ascension (J2000)
2
0
HI column

position-position-velocity structure of the Perseus cloud

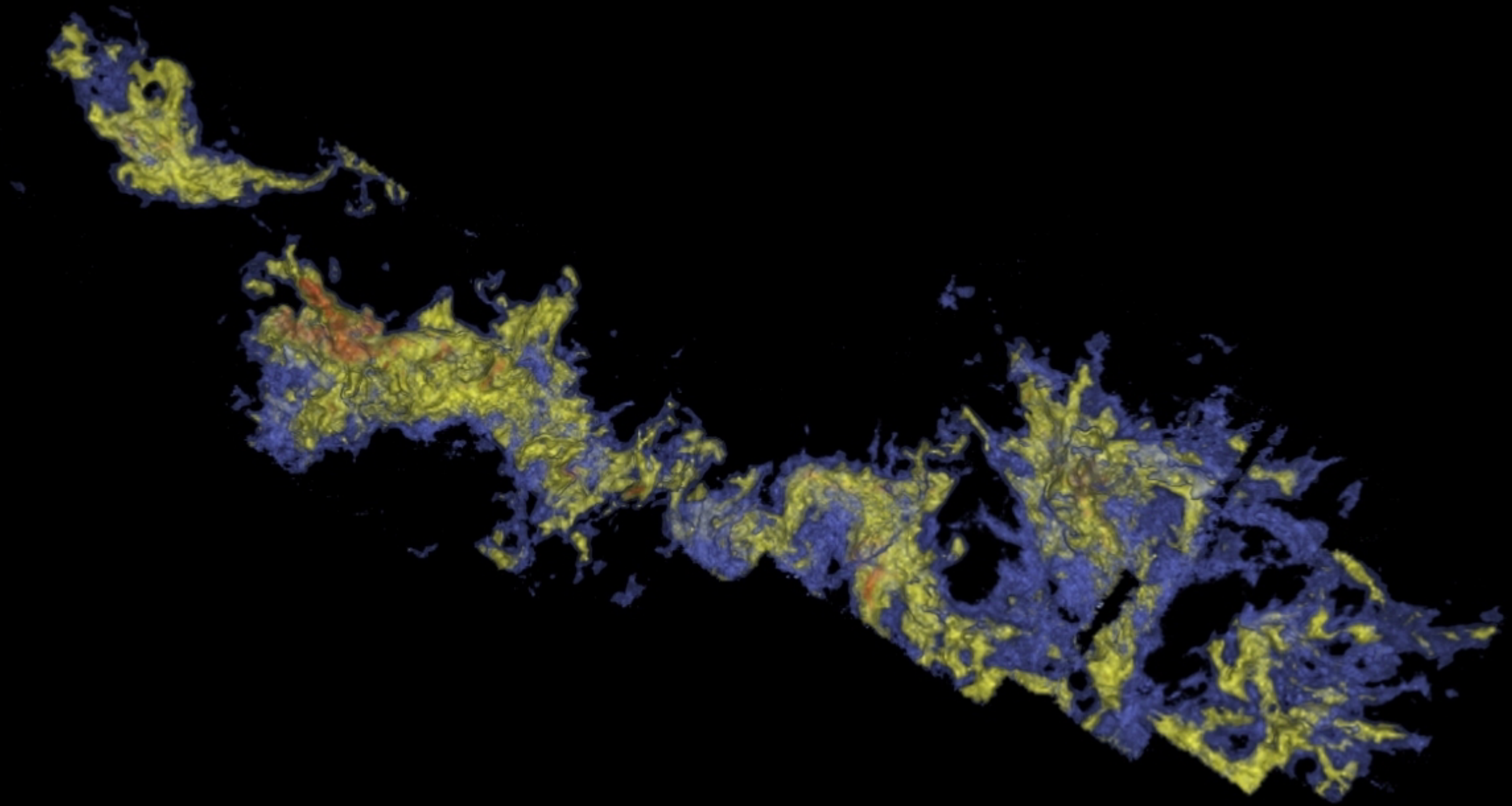

image from Alyssa Goodman: COMPLETE survey

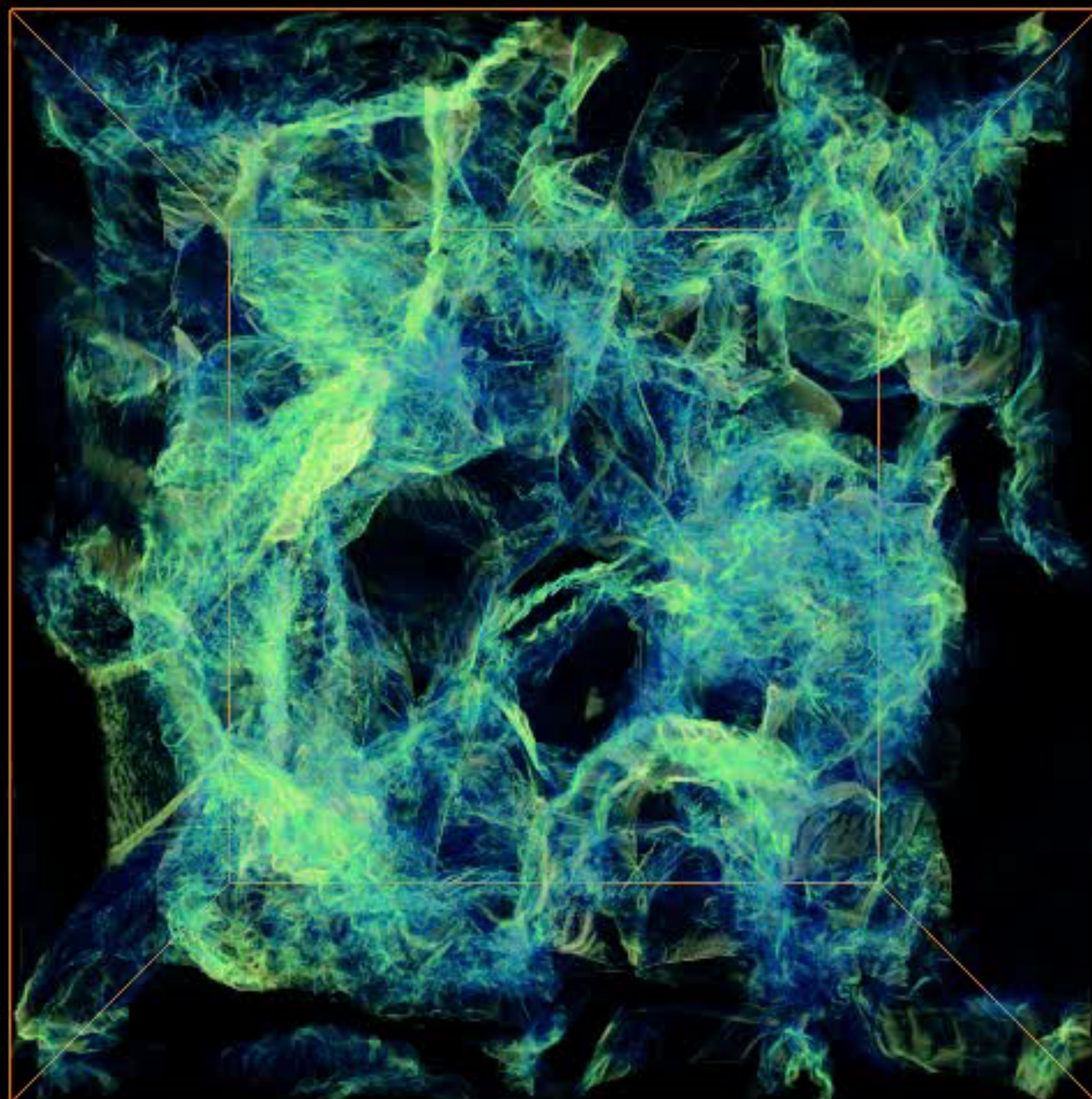

Schmidt et al. (2009, A&A, 494, 127)

caveat of numerical simulations

- most astrophysical turbulence simulations use an ***LES*** approach to model the flow
- principal problem: only large scale flow properties
  - Reynolds number: Re = LV/ν ***(Re_{nature} >> Re_{model})***
  - dynamic range much smaller than true physical one
  - need *subgrid model* (often only dissipation)
  - but what to do for more complex when processes on subgrid scale determine large-scale dynamics
    (chemical reactions, nuclear burning, etc)
  - Turbulence is "space filling" --> difficulty for AMR (don't know what criterion to use for refinement)
- how *large* a Reynolds number do we need to catch basic dynamics right?

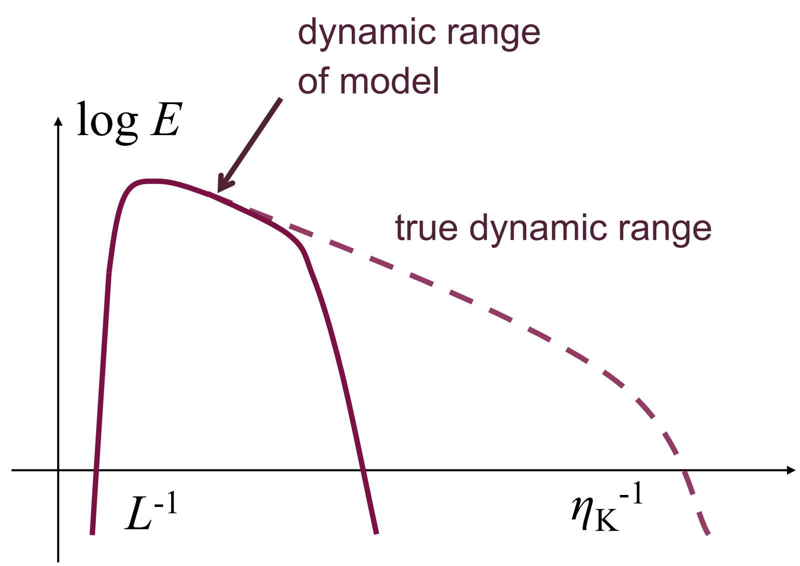

including detailed chemistry

experimental set-up

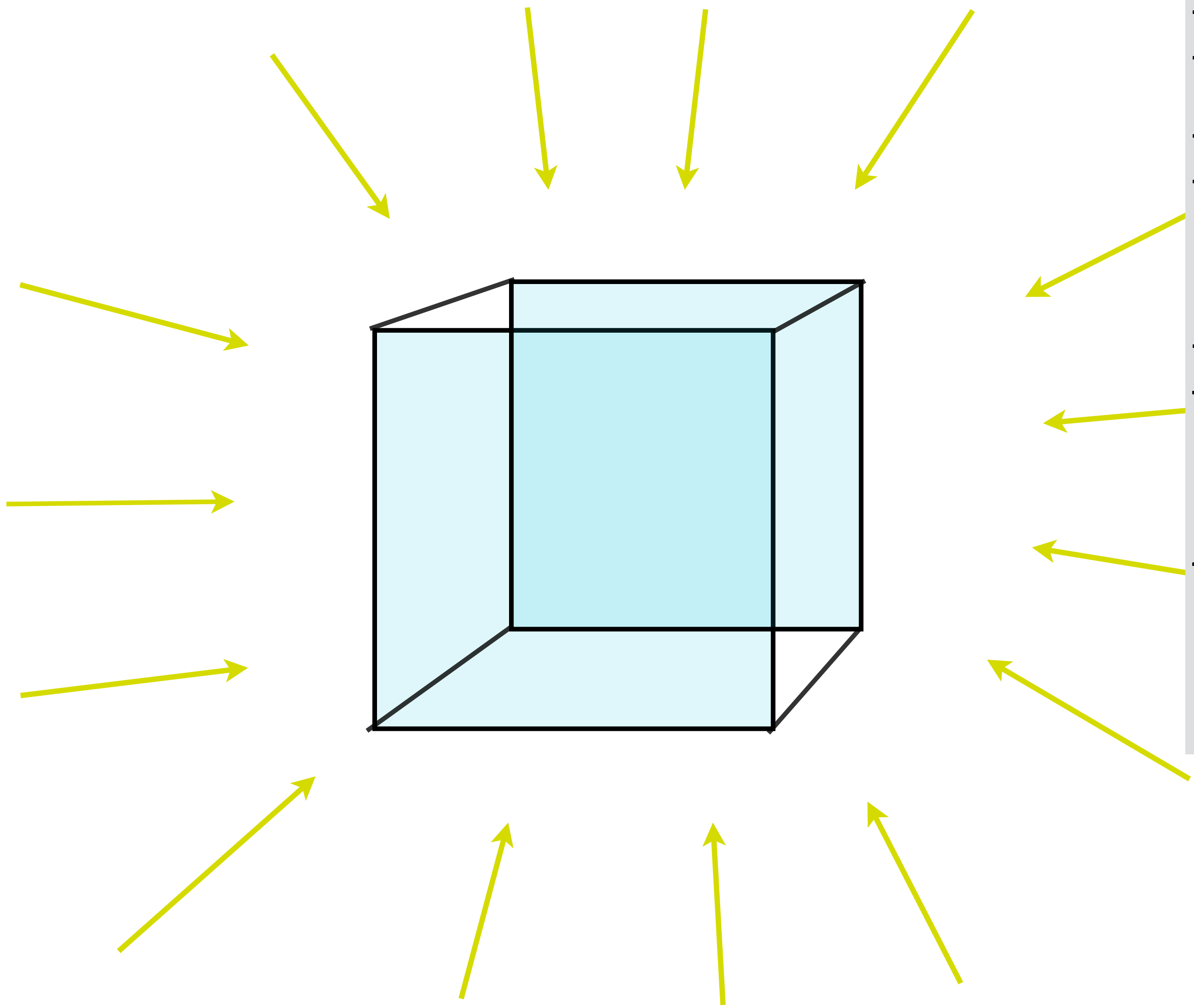

- Arepo and FLASH
- stochastic forcing
  (Ornstein-Uhlenbeck)
- self-gravity
- time-dependent chemistry
  (DVODE, standard variable-coefficient ordinary differential equation solver)
- cooling & heating processes
- gives you mathematically well defined boundary conditions
  --> good for statistical studies
- gives external radiation with TreeCol (a new approximative scheme to calculate column densities from the gravity solver)

chemical model 0

- 32 chemical species
  - 17 in instantaneous equilibrium:

H^-, H_2^+, H_3^+, CH^+, CH_2^+, OH^+, H_2O^+, H_3O^+, CO^+, HOC^+, O^-, C^- and O_2^+

  - 19 full non-equilibrium evolution

e^-, H^+, H, H_2, He, He^+, C, C^+, O, O^+, OH, H_2O, CO,

C_2, O_2, HCO^+, CH, CH_2 and CH_3^+

- 218 reactions
- various heating and cooling processes

long series of publications by Simon Glover and collaborators, e.g. Glover & Mac Low (2007ab), Glover, Federrath, Mac Low, Klessen (2010), Glover & Clark (2012, 2013), Clark & Clover (2012, 2013)

chemical model 1

Process	Reference(s)
Cooling:	
C fine structure lines	Atomic data – Silva & Viegas (2002)
	Collisional rates (H) – Abrahamsson, Krems & Dalgarno (2007)
	Collisional rates (H_2) – Schroder et al. (1991)
	Collisional rates (e^-) – Johnson et al. (1987)
	Collisional rates (H^+) – Roueff & Le Bourlot (1990)
C^+ fine structure lines	Atomic data – Silva & Viegas (2002)
	Collisional rates (H_2) – Flower & Launay (1977)
	Collisional rates (H, $T < 2000$ K) – Hollenbach & McKee (1989)
	Collisional rates (H, $T > 2000$ K) – Keenan et al. (1986)
	Collisional rates (e^-) – Wilson & Bell (2002)
O fine structure lines	Atomic data – Silva & Viegas (2002)
	Collisional rates (H) – Abrahamsson, Krems & Dalgarno (2007)
	Collisional rates (H_2) – see Glover & Jappsen (2007)
	Collisional rates (e^-) – Bell, Berrington & Thomas (1998)
	Collisional rates (H^+) – Pequignot (1990, 1996)
H_2 rovibrational lines	Le Bourlot, Pineau des Forêts & Flower (1999)
CO and H_2O rovibrational lines	Neufeld & Kaufman (1993); Neufeld, Lepp & Melnick (1995)
OH rotational lines	Pavlovski et al. (2002)
Gas-grain energy transfer	Hollenbach & McKee (1989)
Recombination on grains	Wolfire et al. (2003)
Atomic resonance lines	Sutherland & Dopita (1993)
H collisional ionization	Abel et al. (1997)
H_2 collisional dissociation	See Table B1
Compton cooling	Cen (1992)
Heating:	
Photoelectric effect	Bakes & Tielens (1994); Wolfire et al. (2003)
H_2 photodissociation	Black & Dalgarno (1977)
UV pumping of H_2	Burton, Hollenbach & Tielens (1990)
H_2 formation on dust grains	Hollenbach & McKee (1989)
Cosmic ray ionization	Goldsmith & Langer (1978)

(Glover, Federrath, Mac Low, Klessen, 2010, MNRS, 404, 2)

chemical model 2

Table B1. List of collisional gas-phase reactions included in our chemical model.

No.	Reaction	Rate coefficient ($cm^3 s^{-1}$)	Notes	Ref.
1	$H + e^- \rightarrow H^- + \gamma$	$k_1 = \mathrm{dex}[-17.845 + 0.762 \log T + 0.1523 (\log T)^2$		1
		$- 0.03274 (\log T)^3]$	$T \leqslant 6000$ K	
		$= \mathrm{dex}[-16.420 + 0.1998 (\log T)^2$		
		$- 5.447 \times 10^{-3} (\log T)^4$		
		$+ 4.0415 \times 10^{-5} (\log T)^6]$	$T > 6000$ K	
2	$H^- + H \rightarrow H_2 + e^-$	$k_2 = 1.5 \times 10^{-9}$	$T \leqslant 300$ K	2
		$= 4.0 \times 10^{-9} T^{-0.17}$	$T > 300$ K	
3	$H + H^+ \rightarrow H_2^+ + \gamma$	$k_3 = \mathrm{dex}[-19.38 - 1.523 \log T$		3
		$+ 1.118 (\log T)^2 - 0.1269 (\log T)^3]$		
4	$H + H_2^+ \rightarrow H_2 + H^+$	$k_4 = 6.4 \times 10^{-10}$		4
5	$H^- + H^+ \rightarrow H + H$	$k_5 = 2.4 \times 10^{-6} T^{-1/2} (1.0 + T/20000)$		5
6	$H_2^+ + e^- \rightarrow H + H$	$k_6 = 1.0 \times 10^{-8}$	$T \leqslant 617$ K	6
		$= 1.32 \times 10^{-6} T^{-0.76}$	$T > 617$ K	
7	$H_2 + H^+ \rightarrow H_2^+ + H$	$k_7 = [-3.3232183 \times 10^{-7}$		7
		$+ 3.3735382 \times 10^{-7} \ln T$		
		$- 1.4491368 \times 10^{-7} (\ln T)^2$		
		$+ 3.4172805 \times 10^{-8} (\ln T)^3$		
		$- 4.7813720 \times 10^{-9} (\ln T)^4$		
		$+ 3.9731542 \times 10^{-10} (\ln T)^5$		
		$- 1.8171411 \times 10^{-11} (\ln T)^6$		
		$+ 3.5311932 \times 10^{-13} (\ln T)^7]$		
		$\times \exp\left(\frac{-21237.15}{T}\right)$		
8	$H_2 + e^- \rightarrow H + H + e^-$	$k_8 = 3.73 \times 10^{-9} T^{0.1121} \exp\left(\frac{-99430}{T}\right)$		8
9	$H_2 + H \rightarrow H + H + H$	$k_{9,\mathrm{l}} = 6.67 \times 10^{-12} T^{1/2} \exp\left[-\left(1 + \frac{63590}{T}\right)\right]$		9
		$k_{9,\mathrm{h}} = 3.52 \times 10^{-9} \exp\left(-\frac{43900}{T}\right)$		10
		$n_{\mathrm{cr,H}} = \mathrm{dex}\left[3.0 - 0.416 \log\left(\frac{T}{10000}\right) - 0.327 \left\{\log\left(\frac{T}{10000}\right)\right\}^2\right]$		10
10	$H_2 + H_2 \rightarrow H_2 + H + H$	$k_{10,\mathrm{l}} = \frac{5.996 \times 10^{-30} T^{4.1881}}{(1.0 + 6.761 \times 10^{-6} T)^{5.6881}} \exp\left(-\frac{54657.4}{T}\right)$		11
		$k_{10,\mathrm{h}} = 1.3 \times 10^{-9} \exp\left(-\frac{53300}{T}\right)$		12
		$n_{\mathrm{cr,H_2}} = \mathrm{dex}\left[4.845 - 1.3 \log\left(\frac{T}{10000}\right) + 1.62 \left\{\log\left(\frac{T}{10000}\right)\right\}^2\right]$		12
11	$H + e^- \rightarrow H^+ + e^- + e^-$	$k_{11} = \exp[-3.271396786 \times 10^1$		13
		$+ 1.35365560 \times 10^1 \ln T_e$		
		$- 5.73932875 \times 10^0 (\ln T_e)^2$		
		$+ 1.56315498 \times 10^0 (\ln T_e)^3$		
		$- 2.87705600 \times 10^{-1} (\ln T_e)^4$		
		$+ 3.48255977 \times 10^{-2} (\ln T_e)^5$		
		$- 2.63197617 \times 10^{-3} (\ln T_e)^6$		
		$+ 1.11954395 \times 10^{-4} (\ln T_e)^7$		
		$- 2.03914985 \times 10^{-6} (\ln T_e)^8]$		
12	$H^+ + e^- \rightarrow H + \gamma$	$k_{12,\mathrm{A}} = 1.269 \times 10^{-13} \left(\frac{315614}{T}\right)^{1.503}$	Case A	14
		$\times \left[1.0 + \left(\frac{604625}{T}\right)^{0.470}\right]^{-1.923}$		
		$k_{12,\mathrm{B}} = 2.753 \times 10^{-14} \left(\frac{315614}{T}\right)^{1.500}$	Case B	14
		$\times \left[1.0 + \left(\frac{115188}{T}\right)^{0.407}\right]^{-2.242}$		
13	$H^- + e^- \rightarrow H + e^- + e^-$	$k_{13} = \exp[-1.801849334 \times 10^1$		13
		$+ 2.36085220 \times 10^0 \ln T_e$		
		$- 2.82744300 \times 10^{-1} (\ln T_e)^2$		
		$+ 1.62331664 \times 10^{-2} (\ln T_e)^3$		
		$- 3.36501203 \times 10^{-2} (\ln T_e)^4$		
		$+ 1.17832978 \times 10^{-2} (\ln T_e)^5$		
		$- 1.65619470 \times 10^{-3} (\ln T_e)^6$		
		$+ 1.06827520 \times 10^{-4} (\ln T_e)^7$		
		$- 2.63128581 \times 10^{-6} (\ln T_e)^8]$		

(Glover, Federrath, Mac Low, Klessen, 2010, MNRS, 404, 2)

chemical model 2

No.	Reaction	Rate	Ref.
88	$H_2 + He^+ \rightarrow He + H_2^+$	$k_{88} = 7.2 \times 10^{-15}$	63
89	$H_2 + He^+ \rightarrow He + H + H^+$	$k_{89} = 3.7 \times 10^{-14} \exp\left(\frac{35}{T}\right)$	63
90	$CH + H^+ \rightarrow CH^+ + H$	$k_{90} = 1.9 \times 10^{-9}$	28
91	[illegible]	[illegible]	28
92	[illegible]	[illegible]	28
93	[illegible]	[illegible]	28
94	$OH + H^+ \rightarrow OH^+ + H$	$k_{94} = 2.1 \times 10^{-9}$	28
95	$OH + He^+ \rightarrow O^+ + He + H$	$k_{95} = 1.1 \times 10^{-9}$	28
96	$H_2O + H^+ \rightarrow H_2O^+ + H$	$k_{96} = 6.9 \times 10^{-9}$	64
97	$H_2O + He^+ \rightarrow OH + He + H^+$	$k_{97} = 2.04 \times 10^{-10}$	65

Table B2. List of photochemical reactions included in our chemical model

No.	Reaction	Optically thin rate (s^{-1})	γ	Ref.
166	$H^- + \gamma \rightarrow H + e^-$	$R_{166} = 7.1 \times 10^{-7}$	0.5	1
167	$H_2^+ + \gamma \rightarrow H + H^+$	$R_{167} = 1.1 \times 10^{-9}$	1.9	2
168	$H_2 + \gamma \rightarrow H + H$	$R_{168} = 5.6 \times 10^{-11}$	See §2.2	3
169	$H_3^+ + \gamma \rightarrow H_2 + H^+$	$R_{169} = 4.9 \times 10^{-13}$	1.8	4
170	$H_3^+ + \gamma \rightarrow H_2^+ + H$	$R_{170} = 4.9 \times 10^{-13}$	2.3	4
171	$C + \gamma \rightarrow C^+ + e^-$			
172	$C^- + \gamma$			
173	$CH + \gamma$			
174	$CH + \gamma$			
175	$CH^+ + \gamma$			
176	$CH_2 + \gamma$			
177	$CH_2 + \gamma$			
178	$CH_2^+ + \gamma$			
179	$CH_3^+ + \gamma$			
180	$CH_3^+ + \gamma$			
181	$C_2 + \gamma$			
182	$O^- + \gamma$			
183	$OH + \gamma$			
184	$OH + \gamma$			
185	$OH^+ + \gamma$			
186	$H_2O + \gamma$			
187	$H_2O + \gamma$			
188	$H_2O^+ + \gamma$			
189	$H_2O^+ + \gamma$			
190	$H_2O^+ + \gamma$			
191	$H_2O^+ + \gamma$			
192	$H_3O^+ + \gamma$			
193	$H_3O^+ + \gamma$			
194	$H_3O^+ + \gamma$			
195	$H_3O^+ + \gamma$			
196	$O_2 + \gamma$			
197	$O_2 + \gamma \rightarrow O + O$	$R_{197} = 7.0 \times 10^{-10}$	1.8	7
198	$CO + \gamma \rightarrow C + O$	$R_{198} = 2.0 \times 10^{-10}$	See §2.2	13

Table B3. List of reactions included in our chemical model that involve cosmic rays or cosmic-ray induced UV emission

No.	Reaction	Rate ($s^{-1} \zeta_H^{-1}$)	Ref.
199	$H + c.r. \rightarrow H^+ + e^-$	$R_{199} = 1.0$	—
200	$He + c.r. \rightarrow He^+ + e^-$	$R_{200} = 1.1$	1
201	$H_2 + c.r. \rightarrow H^+ + H + e^-$	$R_{201} = 0.037$	1
202	$H_2 + c.r. \rightarrow H + H$	$R_{202} = 0.22$	1
203	$H_2 + c.r. \rightarrow H^+ + H^-$	$R_{203} = 6.5 \times 10^{-4}$	1
204	$H_2 + c.r. \rightarrow H_2^+ + e^-$	$R_{204} = 2.0$	1
205	$C + c.r. \rightarrow C^+ + e^-$	$R_{205} = 3.8$	1
206	$O + c.r. \rightarrow O^+ + e^-$	$R_{206} = 5.7$	1
207	$CO + c.r. \rightarrow CO^+ + e^-$	$R_{207} = 6.5$	1
208	$C + \gamma_{c.r.} \rightarrow C^+ + e^-$	$R_{208} = 2800$	2
209	$CH + \gamma_{c.r.} \rightarrow C + H$	$R_{209} = 4000$	3
210	$CH^+ + \gamma_{c.r.} \rightarrow C^+ + H$	$R_{210} = 960$	3
211	$CH_2 + \gamma_{c.r.} \rightarrow CH_2^+ + e^-$	$R_{211} = 2700$	1
212	$CH_2 + \gamma_{c.r.} \rightarrow CH + H$	$R_{212} = 2700$	1
213	$C_2 + \gamma_{c.r.} \rightarrow C + C$	$R_{213} = 1300$	3
214	$OH + \gamma_{c.r.} \rightarrow O + H$	$R_{214} = 2800$	3
215	$H_2O + \gamma_{c.r.} \rightarrow OH + H$	$R_{215} = 5300$	3
216	$O_2 + \gamma_{c.r.} \rightarrow O + O$	$R_{216} = 4100$	3
217	$O_2 + \gamma_{c.r.} \rightarrow O_2^+ + e^-$	$R_{217} = 640$	3
218	$CO + \gamma_{c.r.} \rightarrow C + O$	$R_{218} = 0.21 T^{1/2} x_{H_2} x_{CO}^{-1/2}$	4

(Glover, Federrath, Mac Low, Klessen, 2010, MNRS, 404, 2)

^{12}CO / ^{13}CO ratio

CO chemistry in GMCs

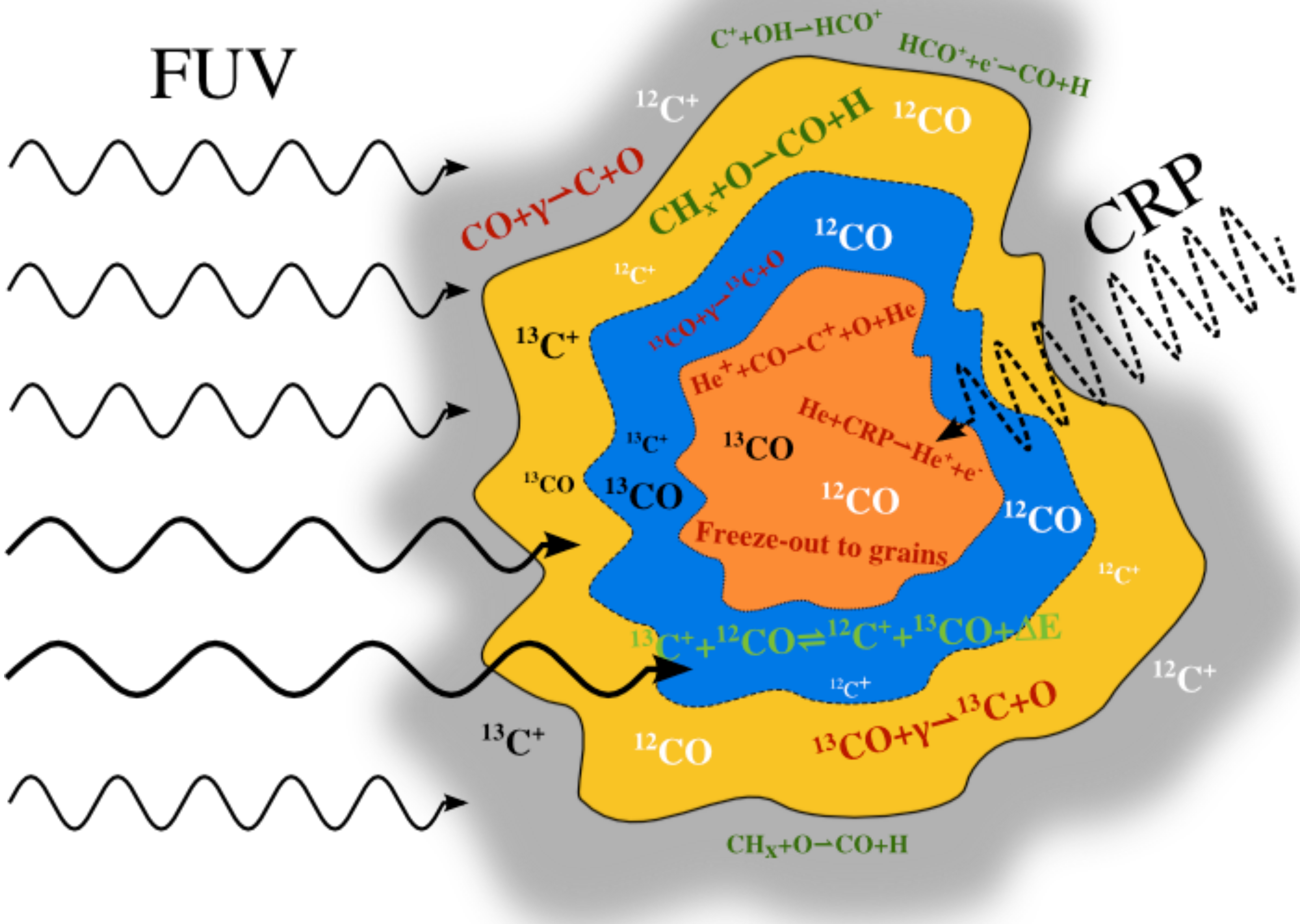

Non-isotope selective reactions

$C^+ + OH \rightarrow HCO^+$ $HCO^+ + e^- \rightarrow H + CO$ $CH_x + O \rightarrow CO + H_x$	**Production**
$He + CRP \rightarrow He^+ + e^-$ $He^+ + CO \rightarrow C^+ + O + He$	**Destruction**
Accretion to grains	**Depletion**

I. Diffuse region ($A_v < 0.5^m$)

$CO + \gamma \rightarrow C + O$

II. Translucent region ($1^m < A < 2^m$)

a) **preferential ^{13}CO photo-dissociation**

b) **Fractionation reaction**

$^{12}CO + ^{13}C \leftarrow\rightarrow ^{13}CO + ^{12}C + 36K$

III. Dense core ($A_v \approx 5^m$)

C^+ depletes

Freeze-out & CRP destruction

(Szücs, Glover, Klessen 2014, MNRAS 445, 4055-4072)

Detailed thermodynamic analysis

6 different models:

Model	n_0 [cm^{-3}]	Metallicity [$Z_\odot$]	ISRF [G_0]	Time [Myr]
a	300	0.3	1	2.046
b	300	0.6	1	1.930
c	300	1	0.1	2.124
d	300	1	1	2.150
e	300	1	10	2.022
f	1000	1	1	0.973

all relevant heating and cooling processes:

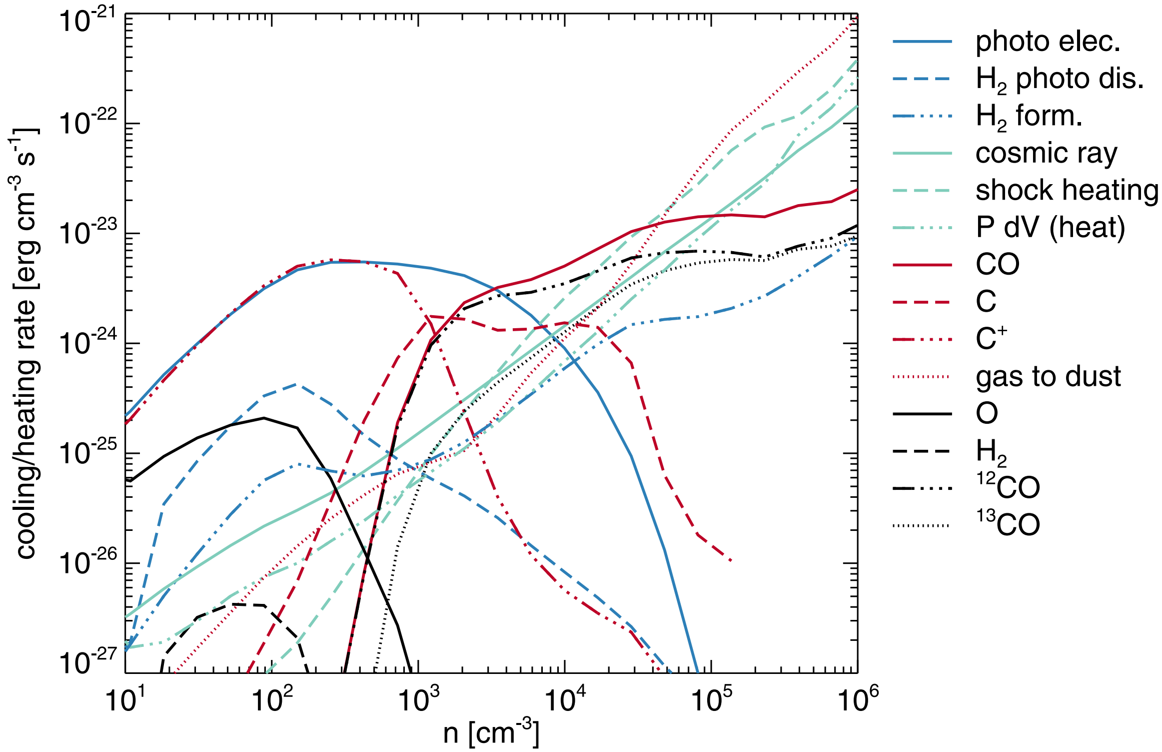

(Szücs et al. 2014, MNRAS 445, 4055)

(also Glover & Clark 2012, MNRAS, 421, 9)

Results – N(^{12}CO)/N(^{13}CO) column densities ratio

N_0 = 300 cm^{-3}
ISRF = 1 G_0
Z = 1 $Z_\odot$
Before first sink particle forms

White contour shows 5×10^{21} cm^{-2}

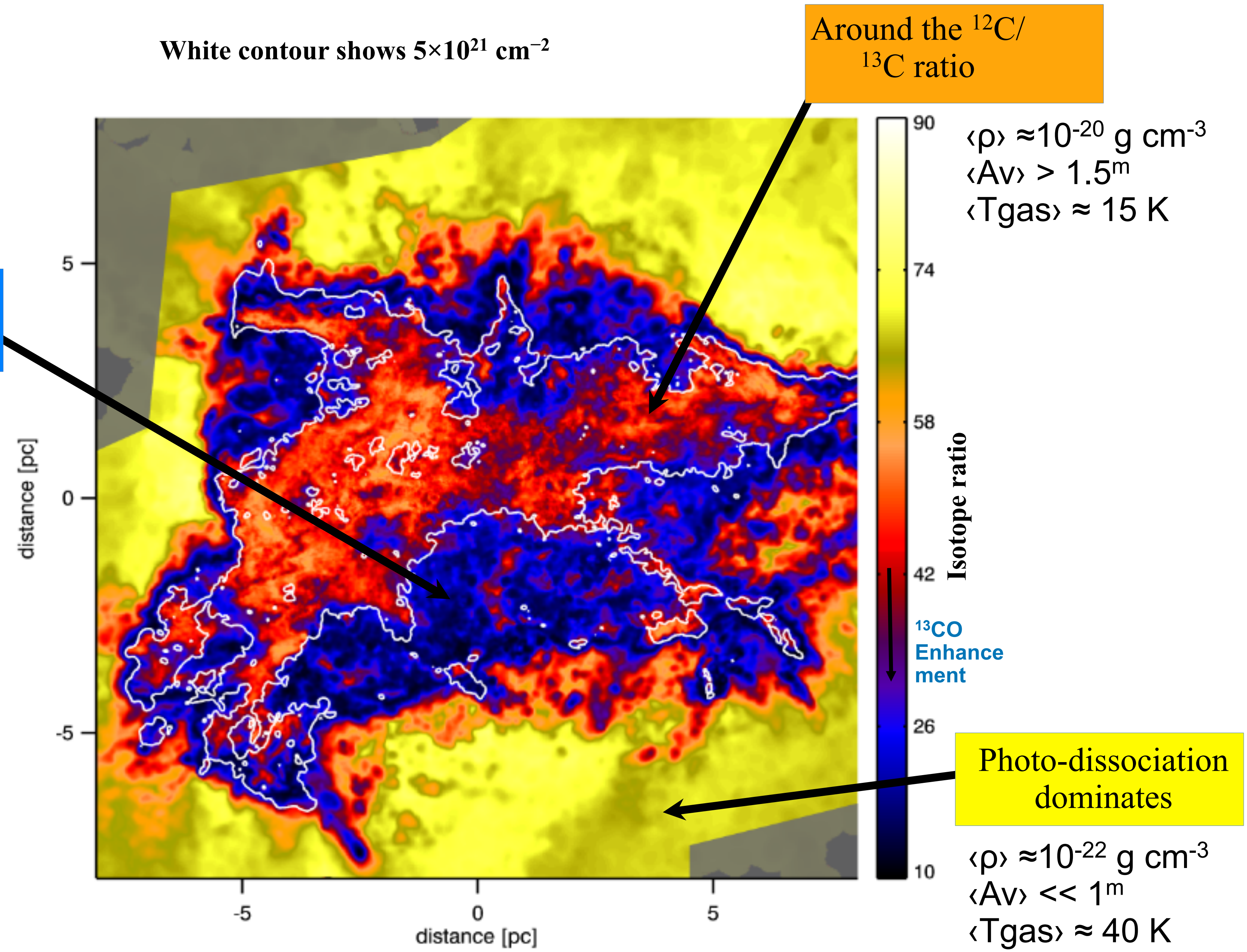

‹ρ› ≈10^{-20} g cm^{-3}
‹Av› > 1.5^m
‹Tgas› ≈ 15 K

‹ρ› ≈10^{-21} g cm^{-3}
‹Av› ≈ 1^m
‹Tgas› ≈ 20 K

‹ρ› ≈10^{-22} g cm^{-3}
‹Av› << 1^m
‹Tgas› ≈ 40 K

(Szücs et al. 2014, MNRAS 445, 4055-4072)

Results – N(^{12}CO)/N(^{13}CO) column densities ratio

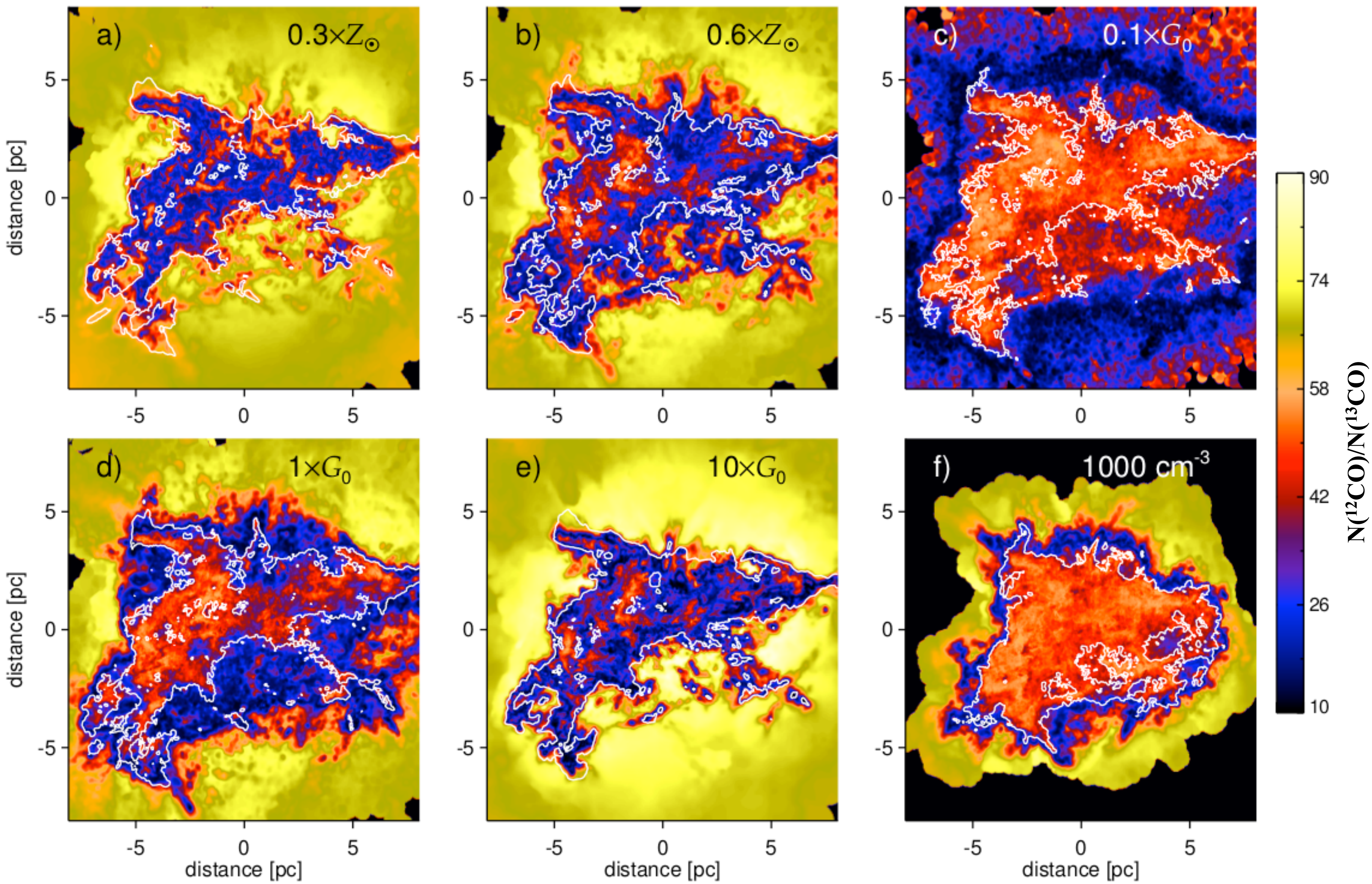

(Szücs et al. 2014, MNRAS 445, 4055-4072)

White contour shows 5×10^{21} cm^{-2}
→ overall density is not changing significantly

Results – N(^{12}CO)/N(^{13}CO) column densities ratio

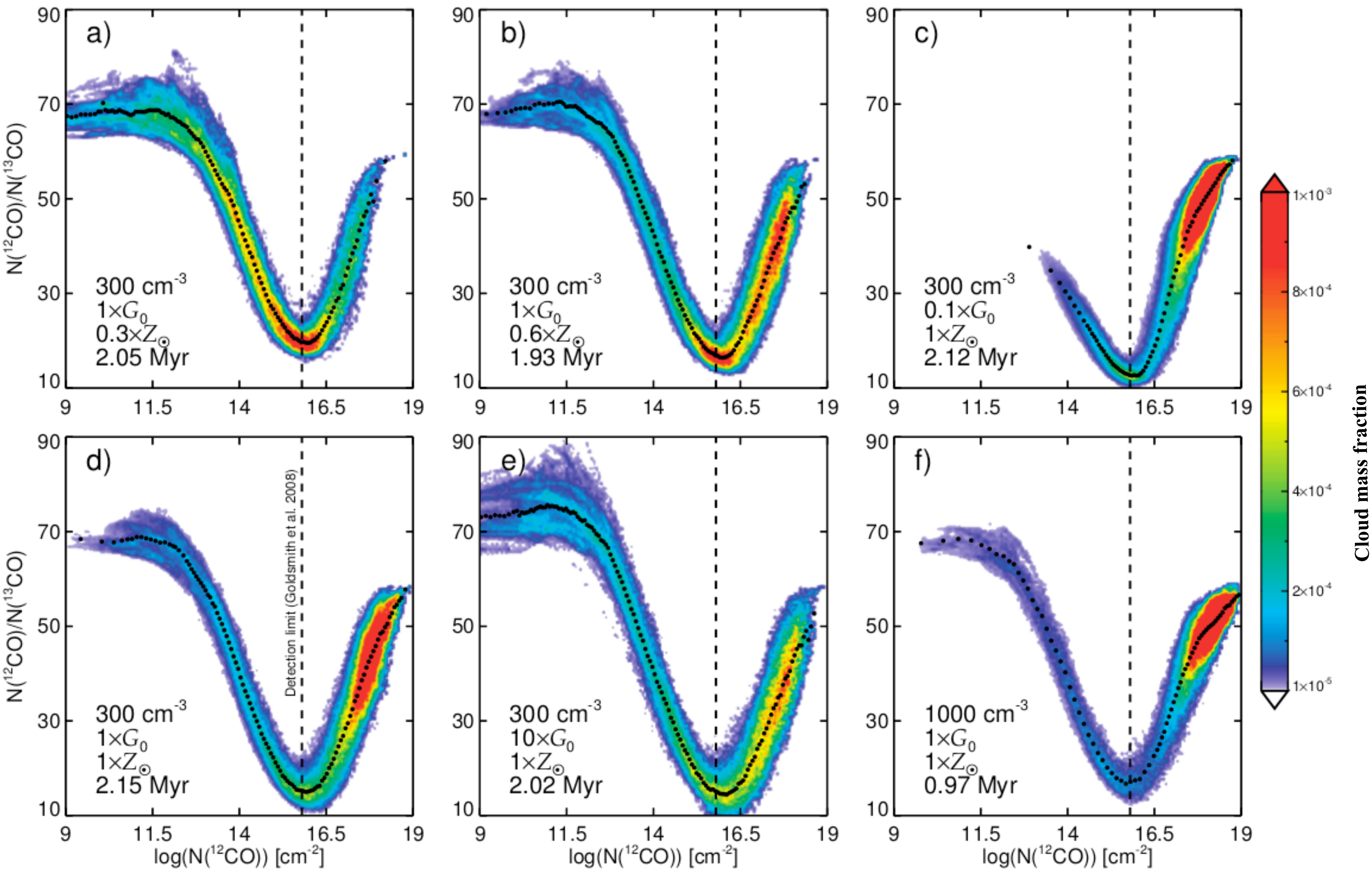

(Szücs et al. 2014, MNRAS 445, 4055-4072)

Fitting formula

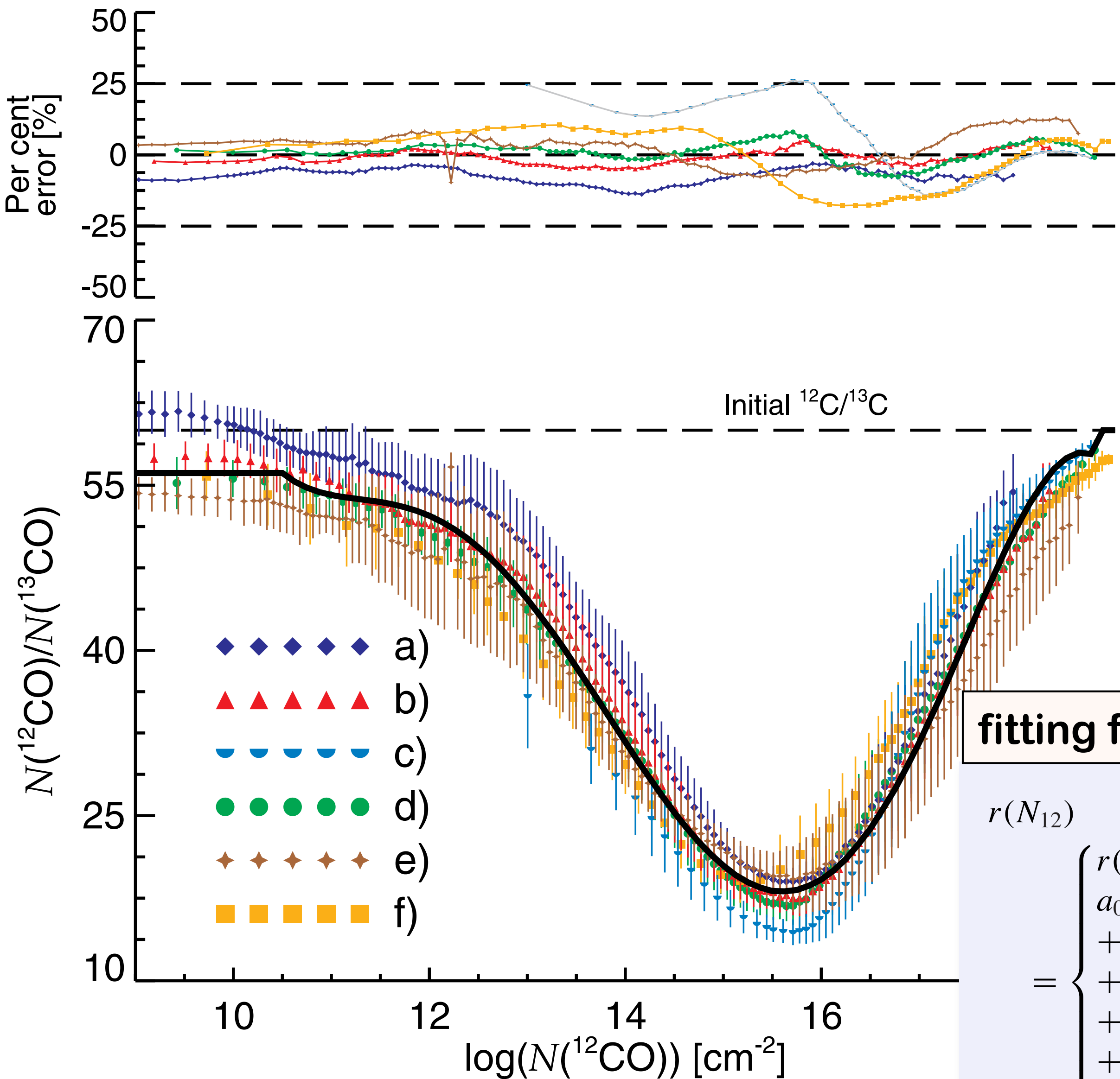

fitting formula:

$$r(N_{12}) = \begin{cases} r(N_{12} = 3.2 \times 10^{10}) & \text{if } N_{12} < 3.2 \times 10^{10} \\ a_{0,12} + a_{1,12}\log_{10}(N_{12}) & \\ +a_{2,12}\log_{10}(N_{12})^2 & \\ +a_{3,12}\log_{10}(N_{12})^3 & \\ +a_{4,12}\log_{10}(N_{12})^4 & \\ +a_{5,12}\log_{10}(N_{12})^5 & \text{if } 3.2 \times 10^{10} \le N_{12} \le 6 \times 10^{18} \\ 60 & \text{if } N_{12} > 6 \times 10^{18} \end{cases}$$

(Szücs et al. 2014, MNRAS 445, 4055-4072)

column density
PDFs

dust emission PDFs

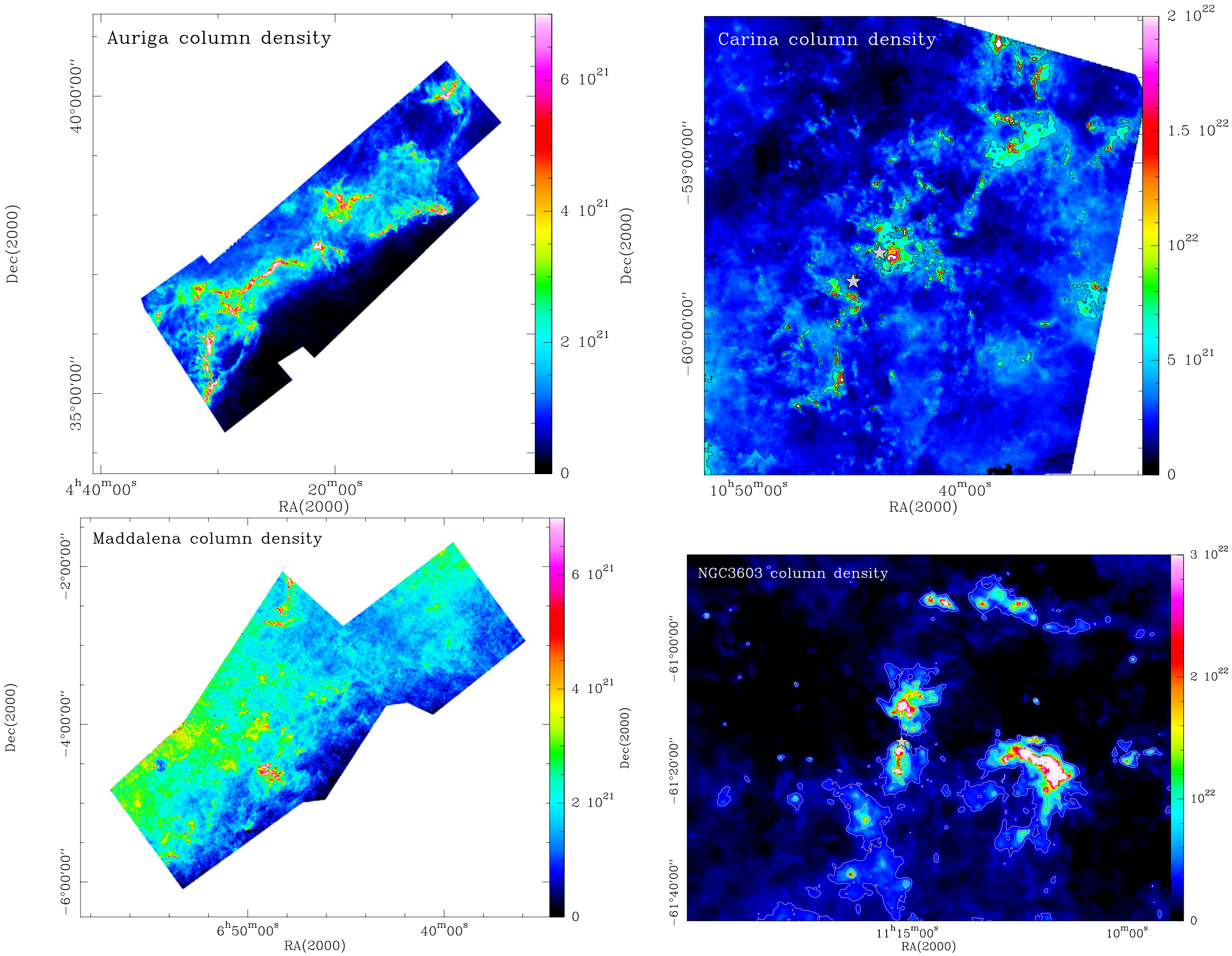

Fig. 1. *Herschel* column density maps (in [cm^{-2}], all starting at zero) of Auriga, Maddalena, NGC 3603, and Carina after correcting for line-of-sight contamination and removing noisy edges and areas where there was no overlap between PACS and SPIRE. The contour levels are 3, 6, 10, and 50×10^{21} cm^{-2} for NGC 3606 and 5, 10, and 20×10^{21} cm^{-2} for Carina.

Schneider et al. 2015, A&A, 575, A79

influence of fore/background

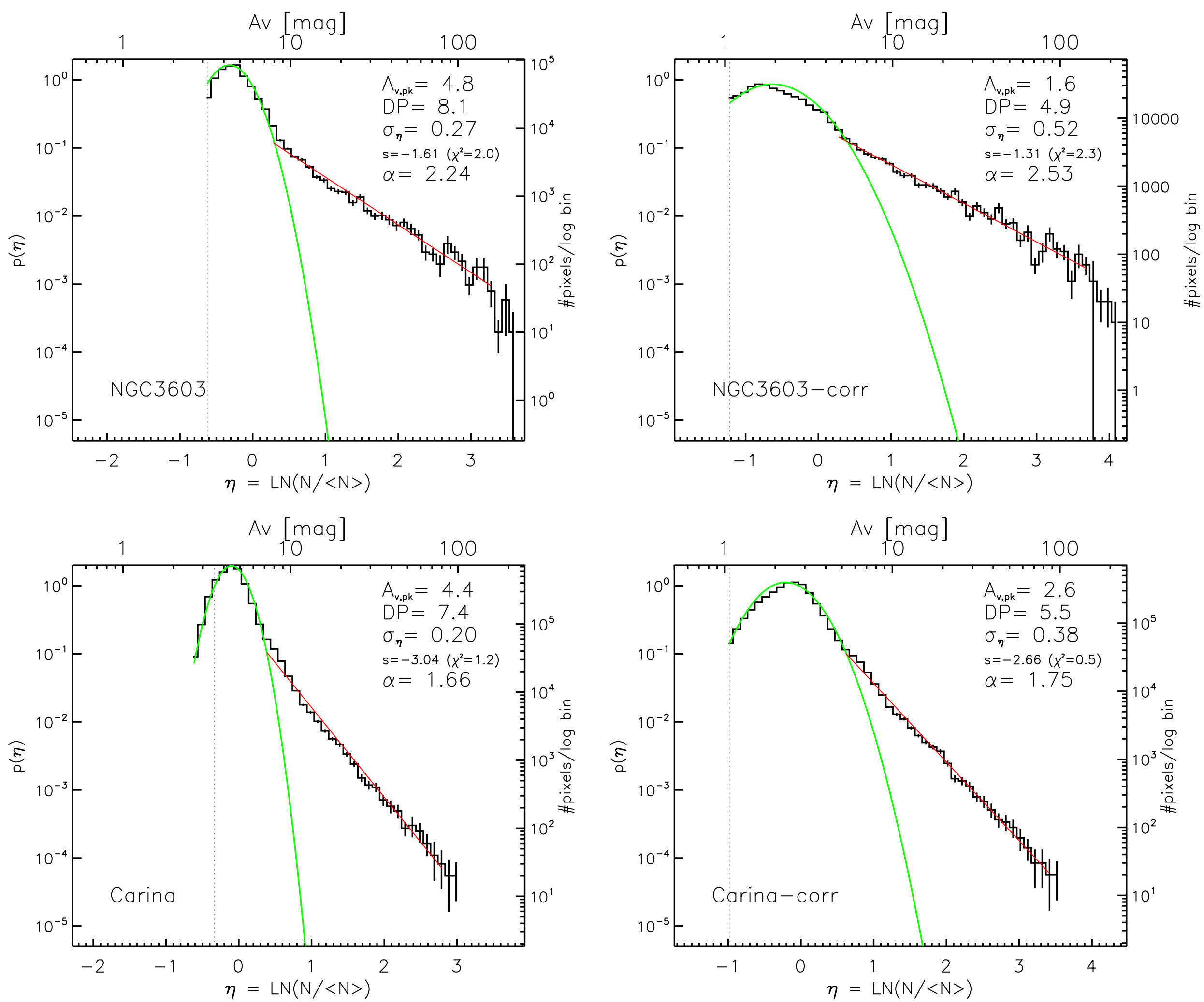

high-mass SF region

results of fore/background correction:

- peak of 'log-normal' shifts to lower Av
- transition from 'log-normal' to power-law shifts to lower Av
- power-law tail remains

Schneider et al. 2015, A&A, 575, A79

influence of fore/background

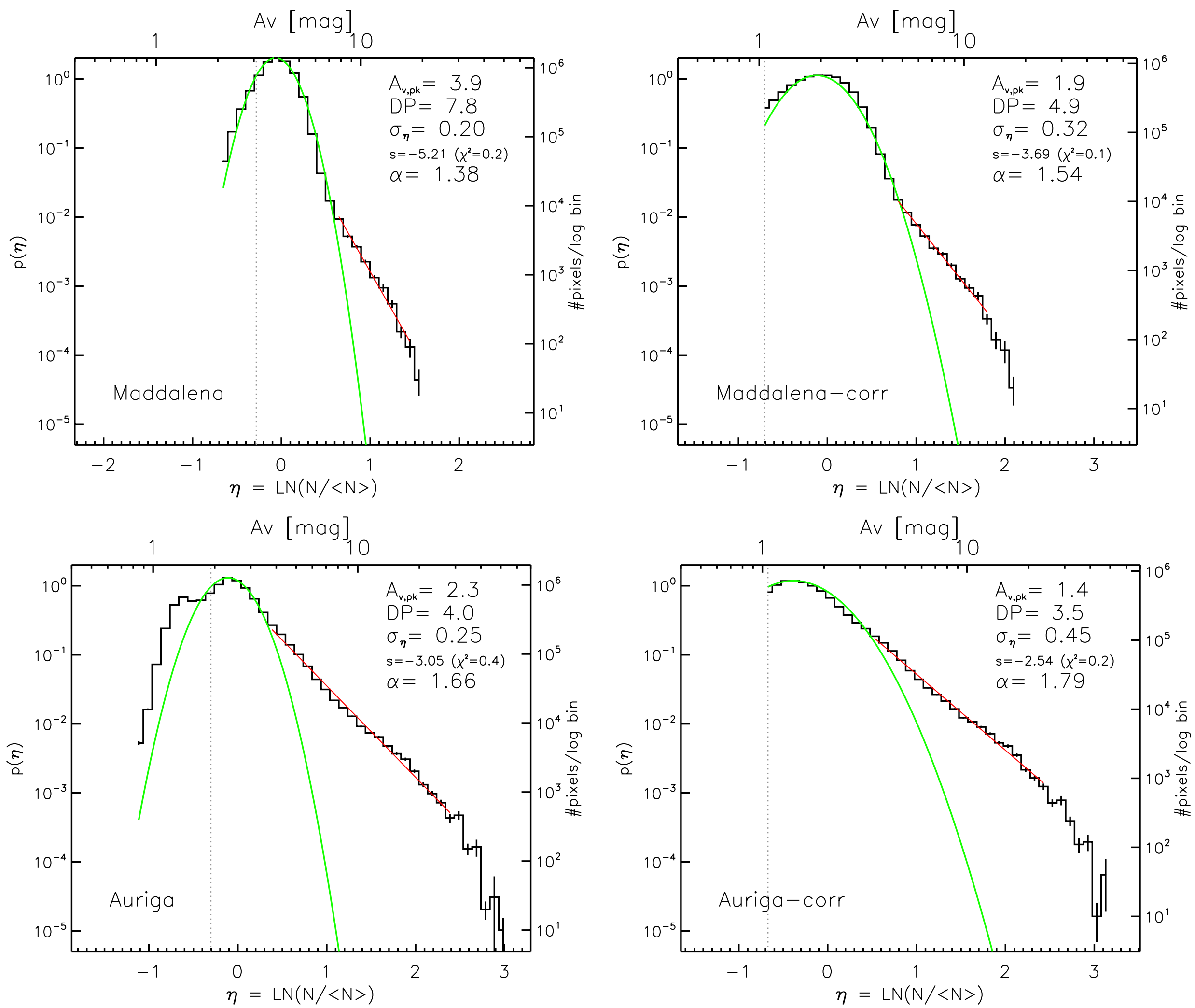

low-mass SF region

results of fore/background correction:

- peak of 'log-normal' shifts to lower Av
- transition from 'log-normal' to power-law shifts to lower Av
- power-law tail remains

Schneider et al. 2015, A&A, 575, A79

detailed analysis on synthetic data

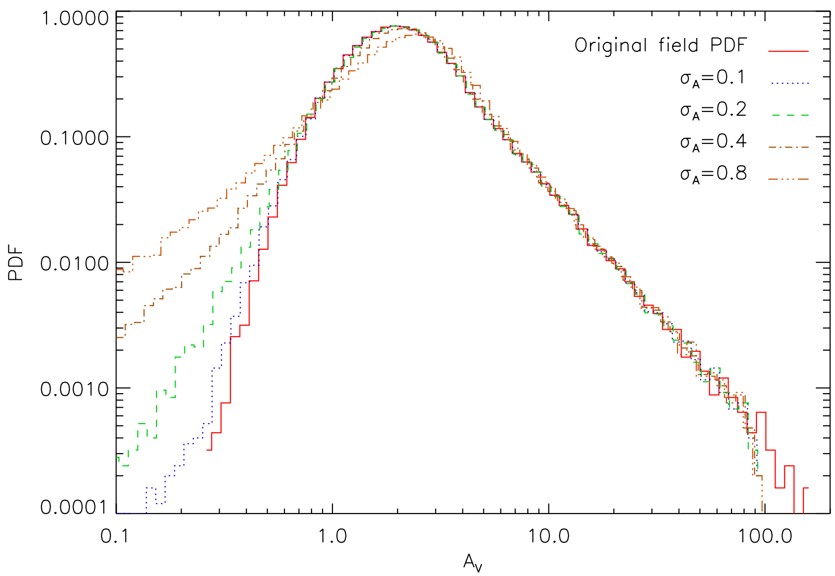

Fig. 8. Simulations of reconstructed PDFs observed with different amplitudes of noise σ_A, expressed in terms of visual extinction. The reconstruction does not depend on the absolute value of the foreground/background contamination.

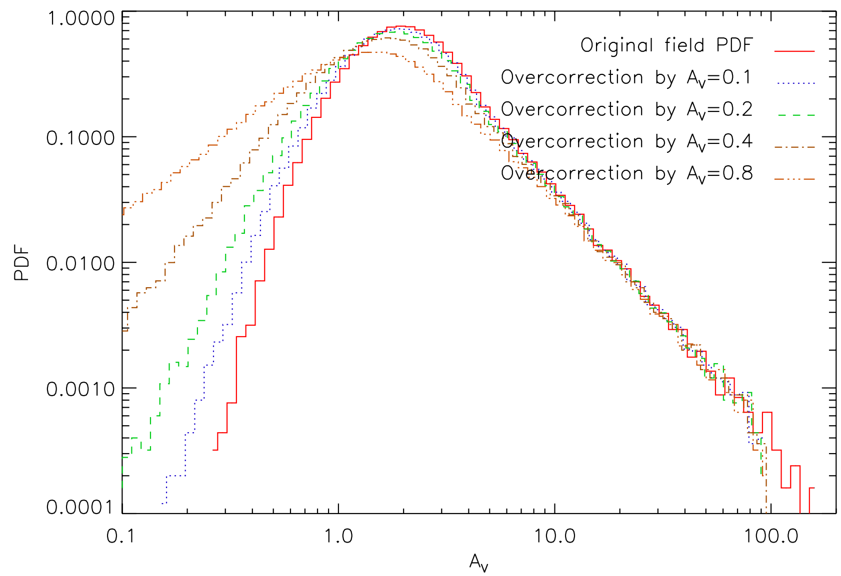

Fig. 9. Simulations of a PDF with negligible noise ($\sigma_A = 0.01$) when applying values that are too high for the contamination correction ΔA_v. The reconstruction does not depend on the absolute value of the foreground/background contamination but only on the difference between actual contamination and subtracted contamination.

different noise levels

influence of 'over correction'

Schneider et al. 2015, A&A, 575, A79

2 examples

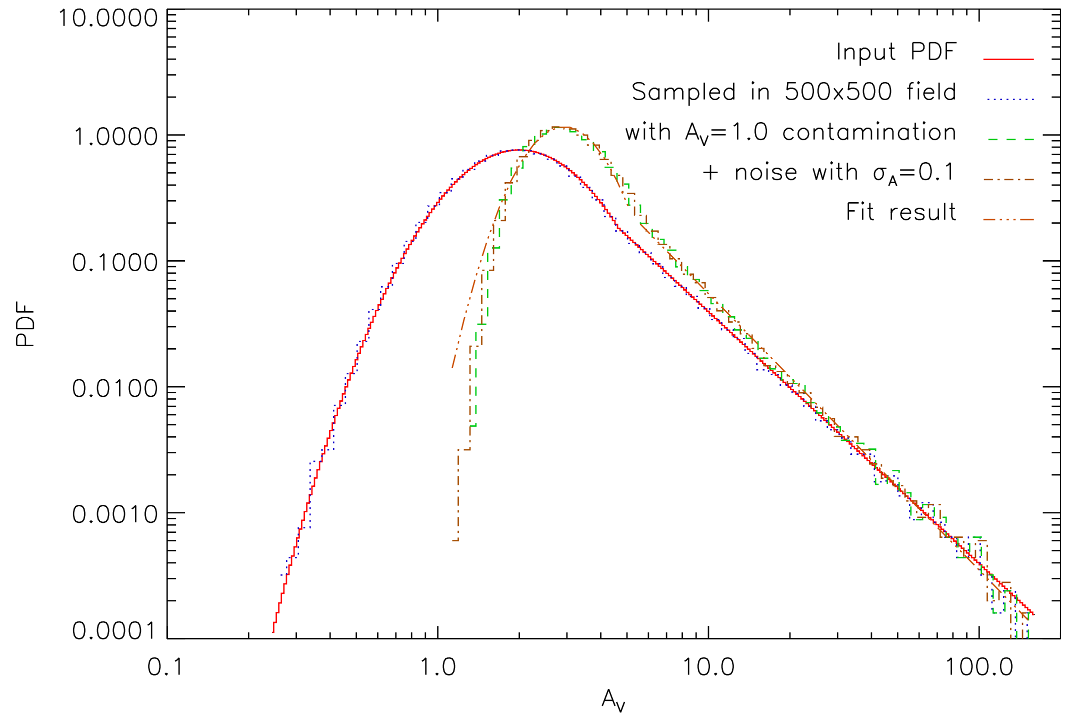

fore/background correction leads to
— flatter power laws
— wider 'log-normal' part
in the standard fitting approach

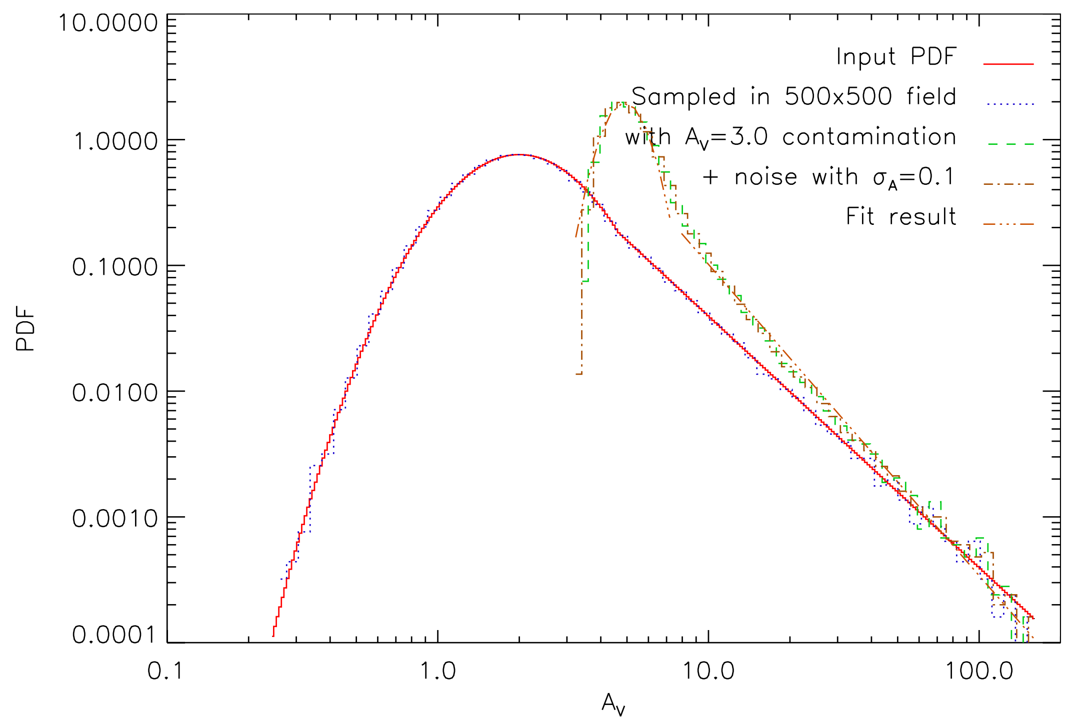

Schneider et al. 2015, A&A, 575, A79

turbulence
and the IMF

different statistical approaches

- there are different quantitative IMF based on turbulence
  - Padoan & Nordlund (2002, 2007)
  - Hennebelle & Chabrier (2008, 2009)
  - Hopkins (2012)
  - all relate the mass spectrum to statistical characteristics of the turbulent velocity fields

The Astrophysical Journal, 684:395–410, 2008 September 1

ANALYTICAL THEORY FOR THE INITIAL MASS FUNCTION: CO CLUMPS AND PRESTELLAR CORES

Patrick Hennebelle
Laboratoire de Radioastronomie, UMR CNRS 8112, École Normale Supérieure et Observatoire de Paris,
24 rue Lhomond, 75231 Paris Cedex 05, France

and

Gilles Chabrier[1]
École Normale Supérieure de Lyon, CRAL, UMR CNRS 5574, Université de Lyon, 69364 Lyon Cedex 07, France
Received 2008 February 12; accepted 2008 May 4

different statistical approaches

- there are different quantitative IMF based on turbulence
    - Padoan & Nordlund (2002, 2007)
    - Hennebelle & Chabrier (2008, 2009)
    - Hopkins (2012)
    - all relate the mass spectrum to statistical characteristics of the turbulent velocity fields

The Astrophysical Journal, 684:395–410, 2008 September 1

The Astrophysical Journal, 702:1428–1442, 2009 September 10
doi:10.1088/0004-637X/702/2/1428

ANALYTICAL THEORY FOR THE INITIAL MASS FUNCTION. II. PROPERTIES OF THE FLOW

Patrick Hennebelle[1] and Gilles Chabrier[2]
[1] Laboratoire de radioastronomie, UMR CNRS 8112, École normale supérieure et Observatoire de Paris, 24 rue Lhomond, 75231 Paris cedex 05, France
[2] École normale supérieure de Lyon, CRAL, UMR CNRS 5574, Université de Lyon, 69364 Lyon Cedex 07, France
Received 2009 April 1; accepted 2009 July 17; published 2009 August 21

different statistical approaches

- there are different quantitative IMF based on turbulence
  - Padoan & Nordlund (2002, 2007)
  - Hennebelle & Chabrier (2008, 2009)
  - Hopkins (2012)
  - all relate the mass spectrum to statistical characteristics of the turbulent velocity fields

The Astrophysical Journal, 684:395–410, 2008 September 1

The Astrophysical Journal, 702:1428–1442, 2009 September 10 doi:10.1088/0004-637X/702/2/1428

ANA ... OW

[1] Laboratoir ... 05, France

Monthly Notices of the ROYAL ASTRONOMICAL SOCIETY
Mon. Not. R. Astron. Soc. **423,** 2037–2044 (2012) doi:10.1111/j.1365-2966.2012.20731.x

The stellar initial mass function, core mass function and the last-crossing distribution

Philip F. Hopkins★
Department of Astronomy, University of California Berkeley, Berkeley, CA 94720, USA

different statistical approaches

- there are different quantitative IMF based on turbulence
  - Padoan & Nordlund (2002, 2007)
  - Hennebelle & Chabrier (2008, 2009)
  - Hopkins (2012)
  - all relate the mass spectrum to statistical characteristics of the turbulent velocity fields

- there are alternative approaches
  - IMF as closest packing problem / *sampling* problem in *fractal* clouds (Larson 1992, 1995, Elmegreen 1997ab, 2000ab, 2002)
  - IMF as purely *statistical* problem (Larson 1973, Zinnecker 1984, 1990, Adams & Fatuzzo 1996)
  - IMF from (proto)stellar *feedback* (Silk 1995, Adams & Fatuzzo 1996)
  - IMF from competitive *coagulation* (Murray & Lin 1995, Bonnell et al. 2001ab, etc.)

caveat: everybody gets the IMF!

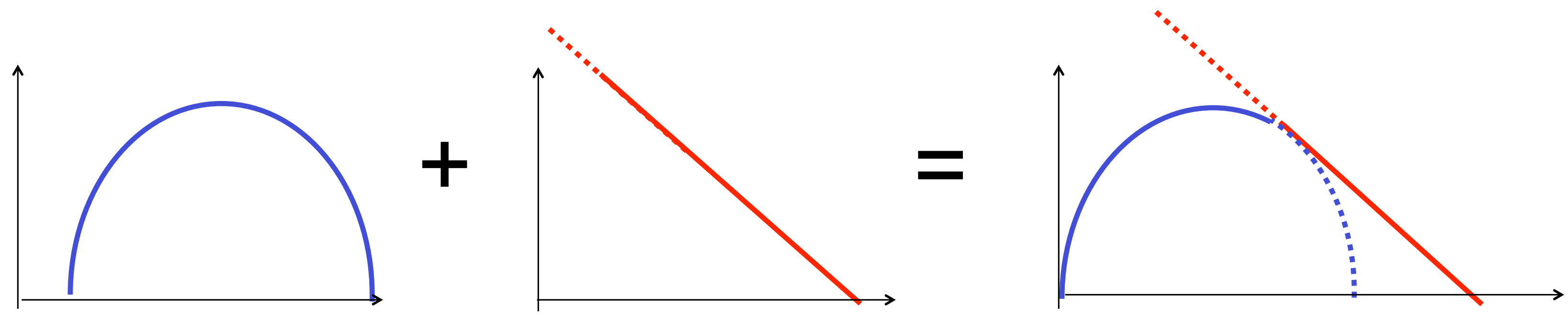

- combine scale free process → *POWER LAW BEHAVIOR*
  - turbulence (Padoan & Nordlund 2002, Hennebelle & Chabrier 2008, Hopkins 2008)
  - gravity in dense clusters (Bonnell & Bate 2006, Klessen 2001)

- with highly stochastic processes → central limit theorem
  → *GAUSSIAN DISTRIBUTION*
  - basically mean thermal Jeans length (or feedback)
  - universality due to dust physics: coupling between dust and gas insensitive to radiation field and metallicity
    (Elmegreen et al. 2008, Omukai et al. 2005)

Offner et al. 2014, Protostars and Planets VI, 53-75
Klessen & Glover 2014, Saas Fee Lecture, arXiv:1412.5182, 1-191

caveat: everybody gets the IMF!

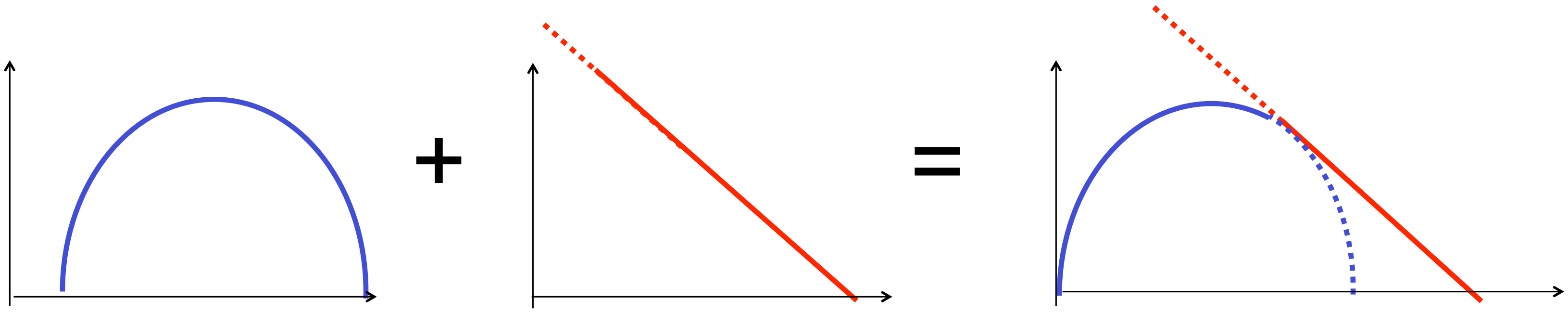

"everyone" gets the right IMF
→ better look for secondary indicators

- *stellar multiplicity*
- protostellar *spin* (including disk)
- *spatial distribution* + *kinematics* in young clusters
- *magnetic field strength* and *orientation*

Offner et al. 2014, Protostars and Planets VI, 53-75
Klessen & Glover 2014, Saas Fee Lecture, arXiv:1412.5182, 1-191

properties of star forming filaments

large-scale filaments

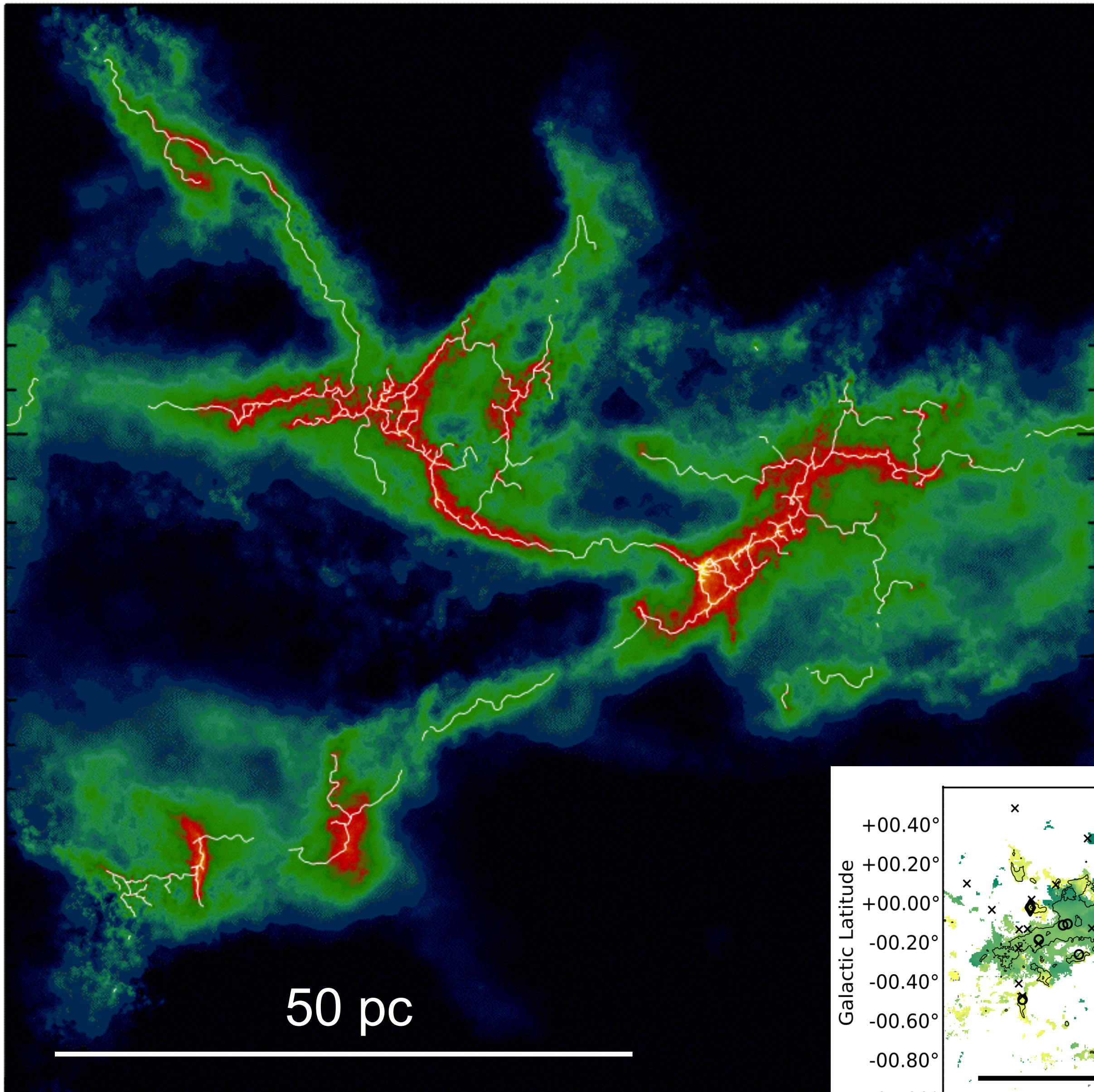

Smith et al. (2014, MNRAS, 445, 2900)

next steps:

studying details of ISM morphology and star formation in dedicated zoom-in simulation

example:
giant molecular cloud complex (~10^6 $M_\odot$) viewed in the plane of the disk.

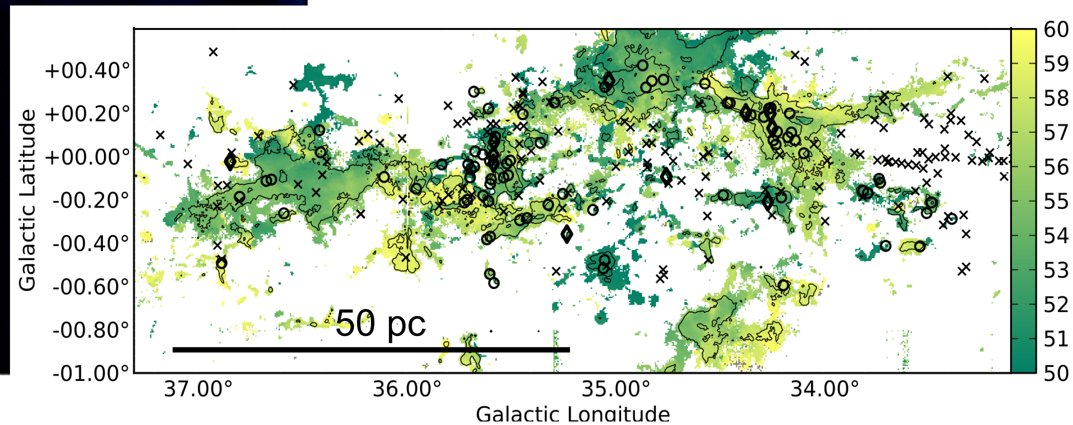

Ragan et al., 2014, A&A submitted, arXiv:1403.1450)

zoom-in on filaments

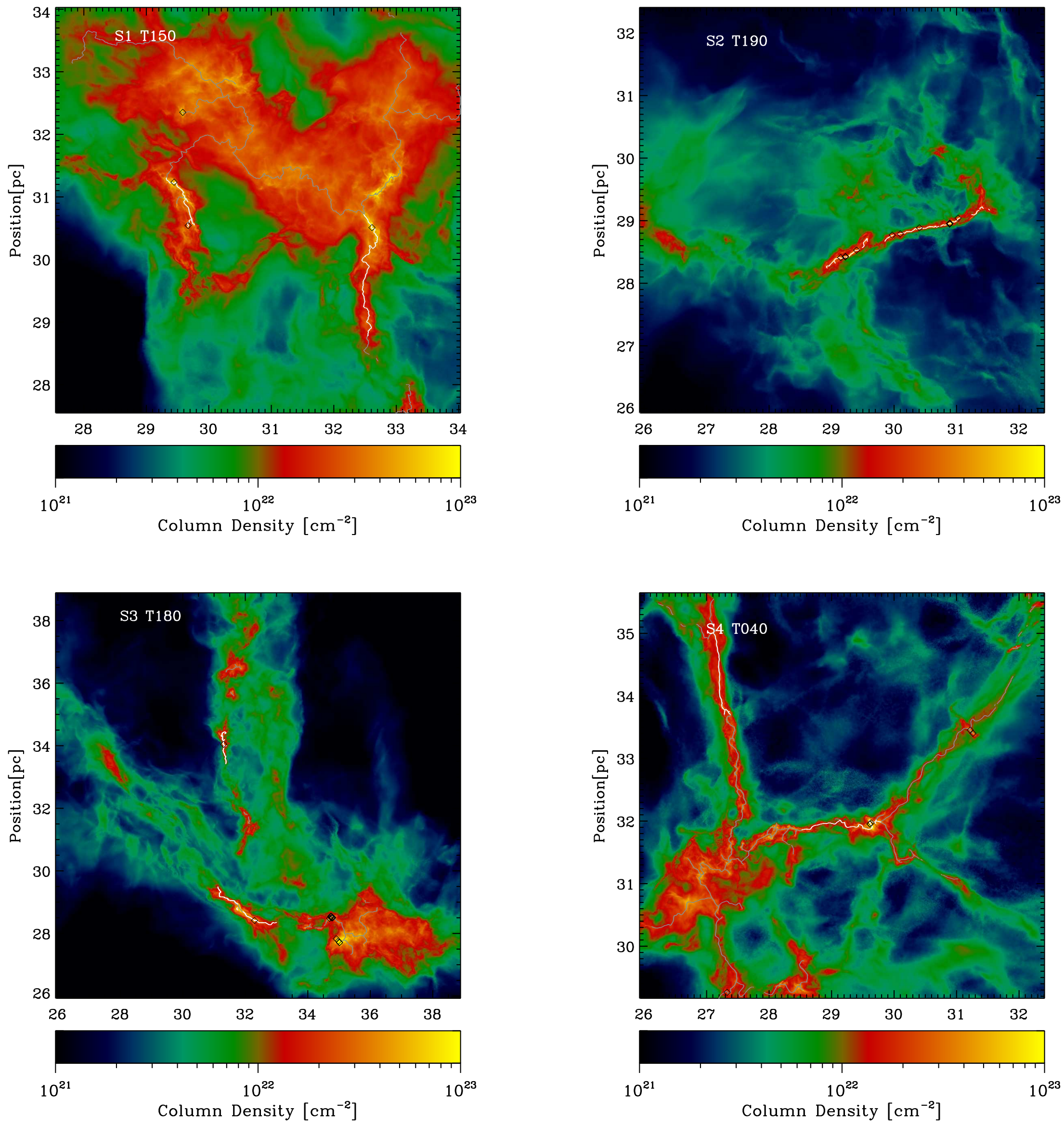

next steps:

studying details of ISM morphology and star formation in dedicated zoom-in simulation *(resolution ≲2000 AU, with full chemistry)*

analysis:

- morphology
- velocity
- chemistry
- observations (dust maps for Herschel, CO, N_2H+, HCN, etc. for line obs.)

Smith et al. (2014, MNRAS, 445, 2900,
also Smith et al. 2012, ApJ, 750, 64, Smith et al. 2013, ApJ, 771, 24, Chira et al., 2014, MNRAS, submitted)

filaments do not have universal width

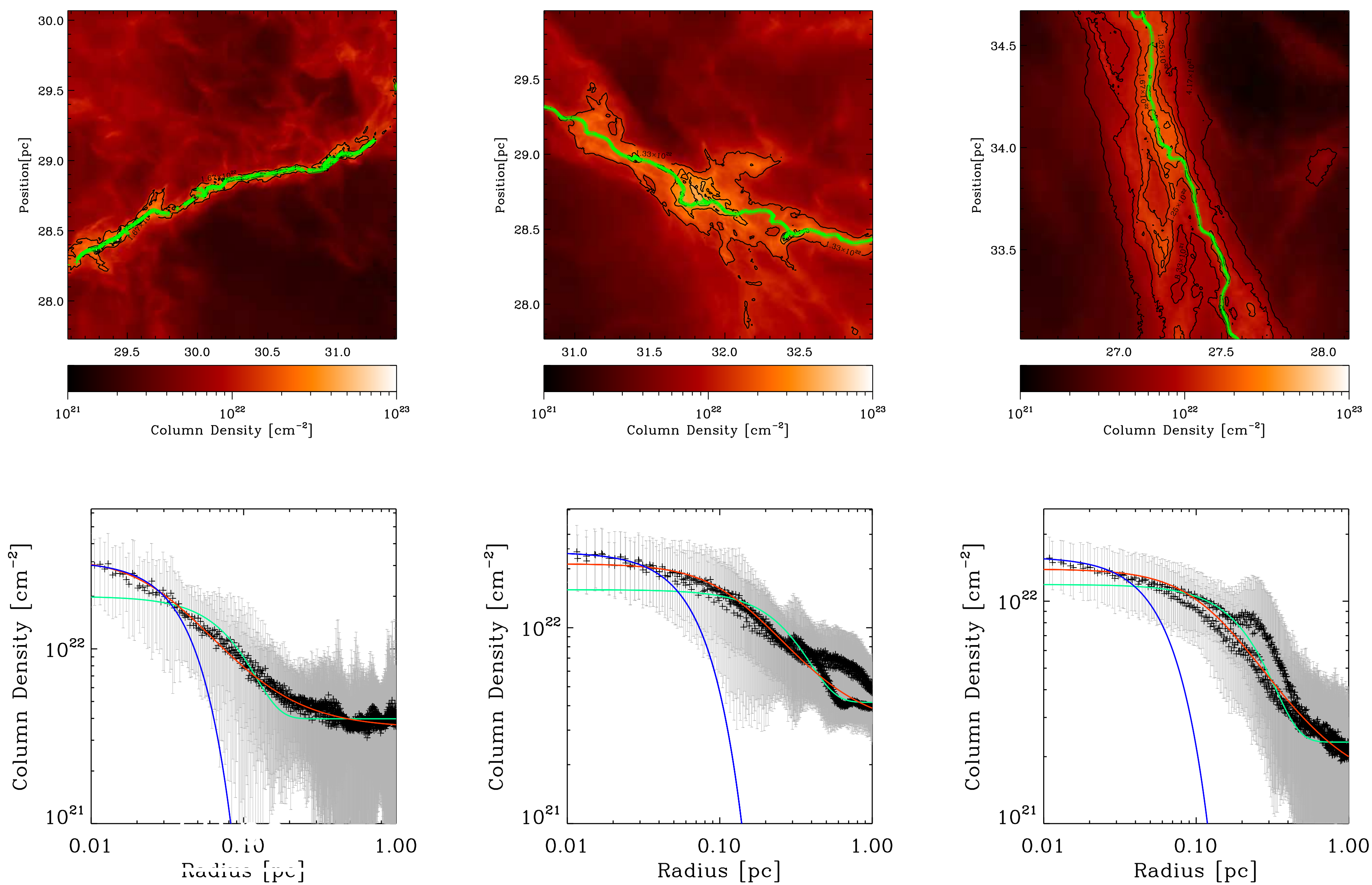

Smith et al. (2014, MNRAS, 445, 2900)

filaments do not have universal width

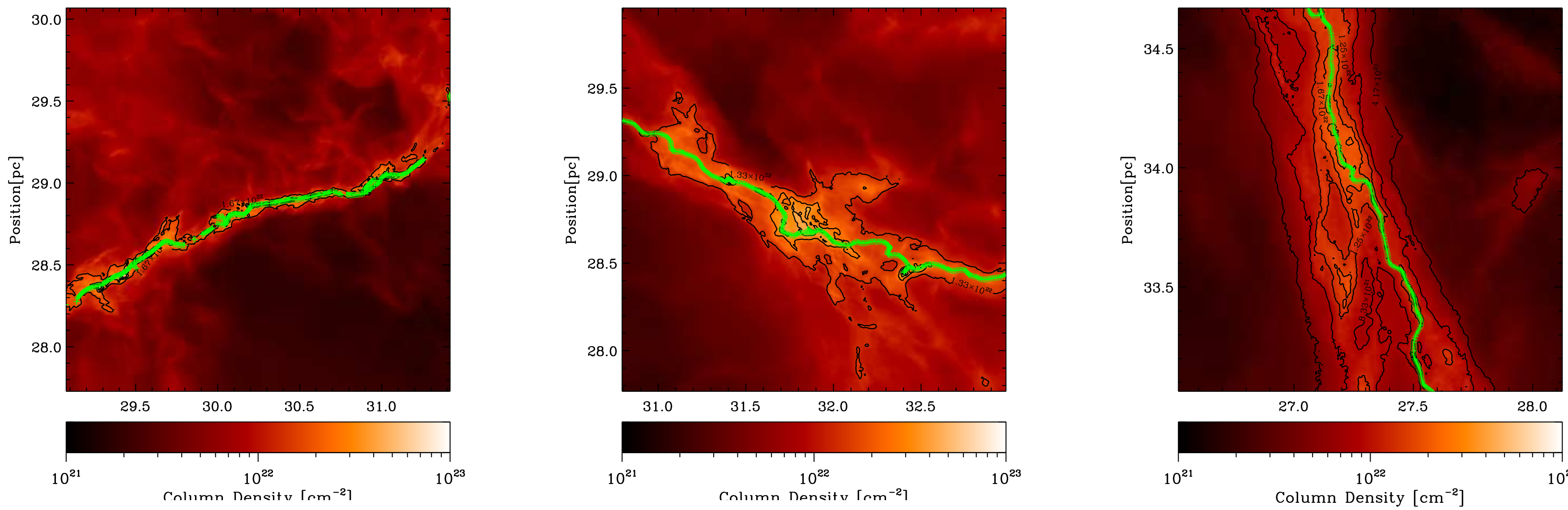

Arzoumanian, et al., 2011, A&A, 529, L6

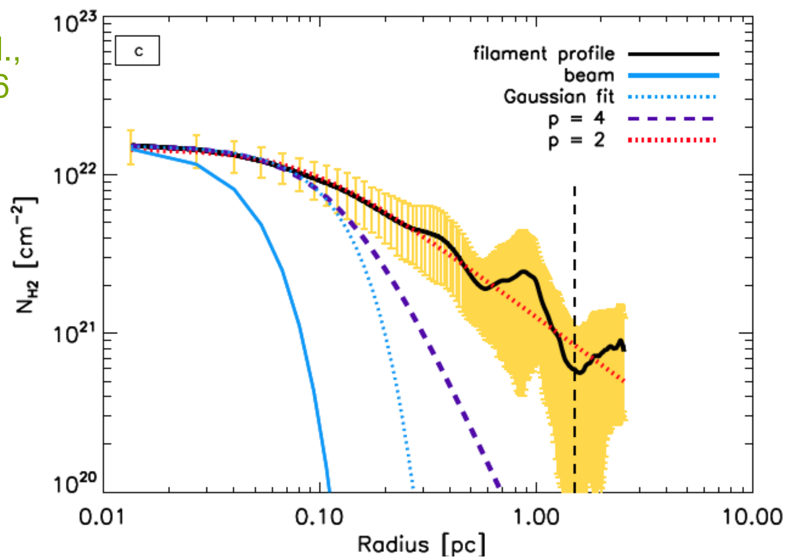

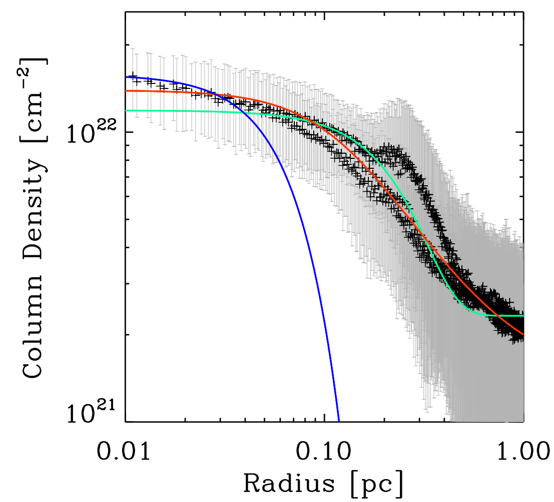

Smith et al. (2014, MNRAS, 445, 2900)

3D filaments have complex structure

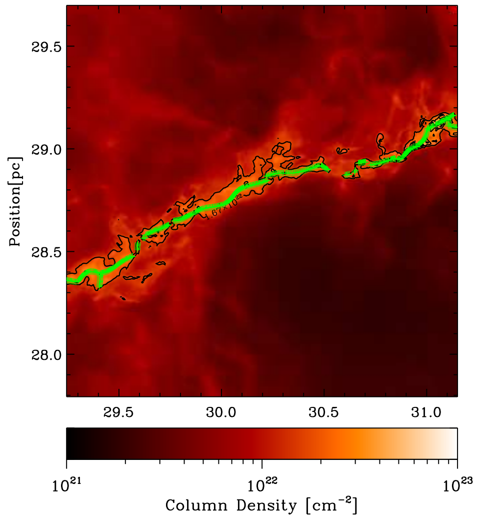

2D filament detection shows nice coherent filament

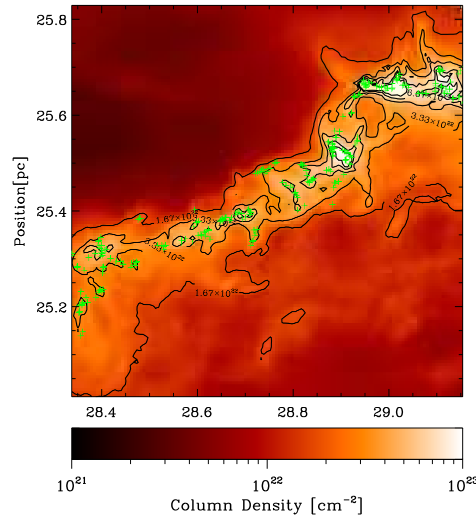

2D + LOS peak detection shows complex structure

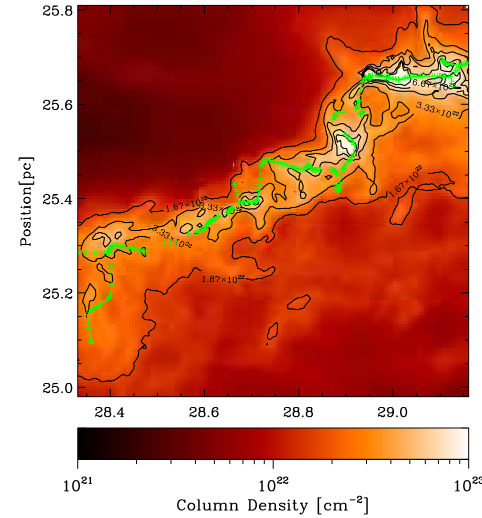

full 3D filament analysis confirms this picture

Smith et al. (2014, MNRAS, 445, 2900)

walk along the filament

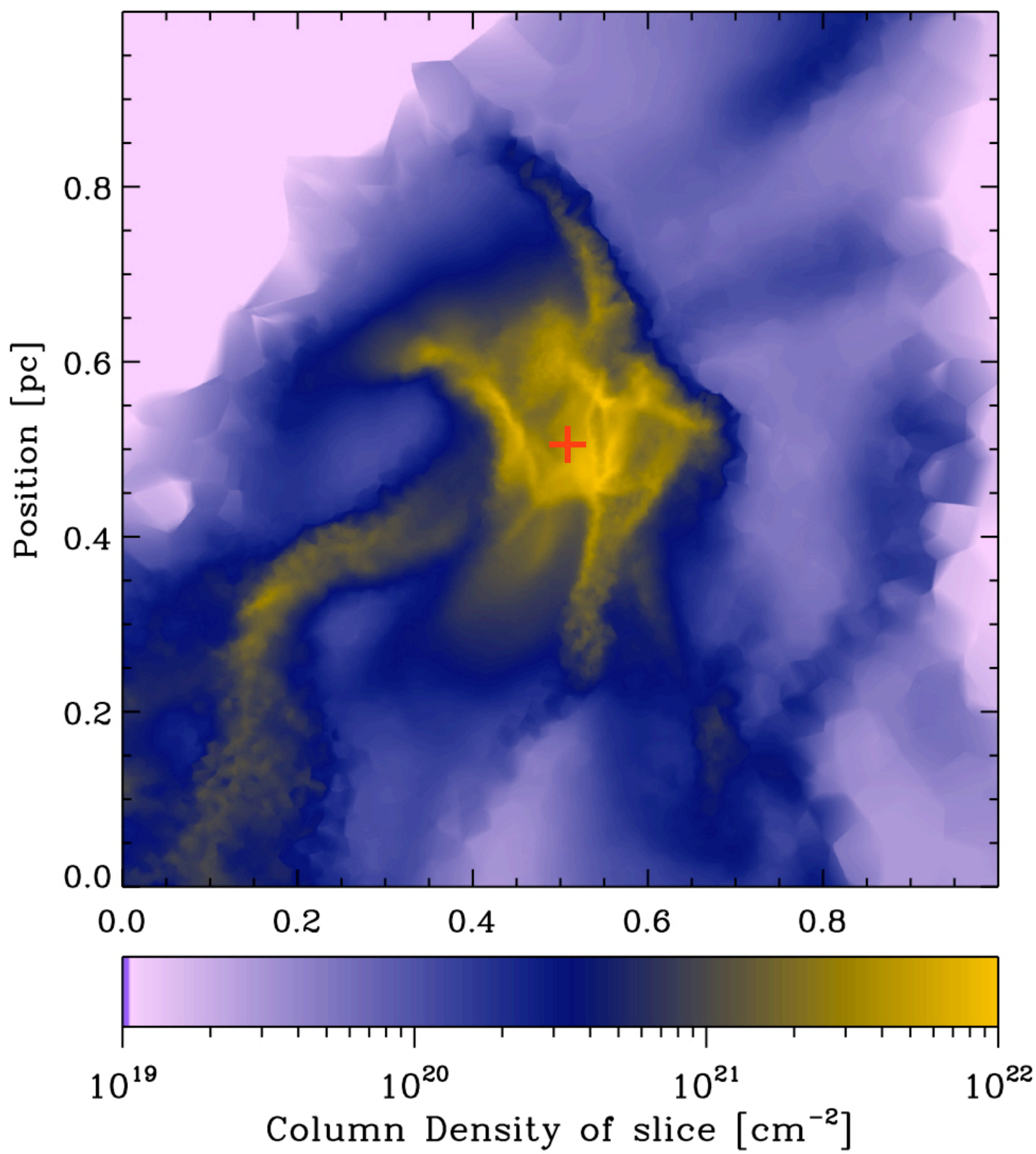

- walking along the filament exhibits complex 3D structure that is now (fully) seen in projected density
- is this similar to the filament fibers proposed by Hacar et al. (2013, A&A, 554, 55)

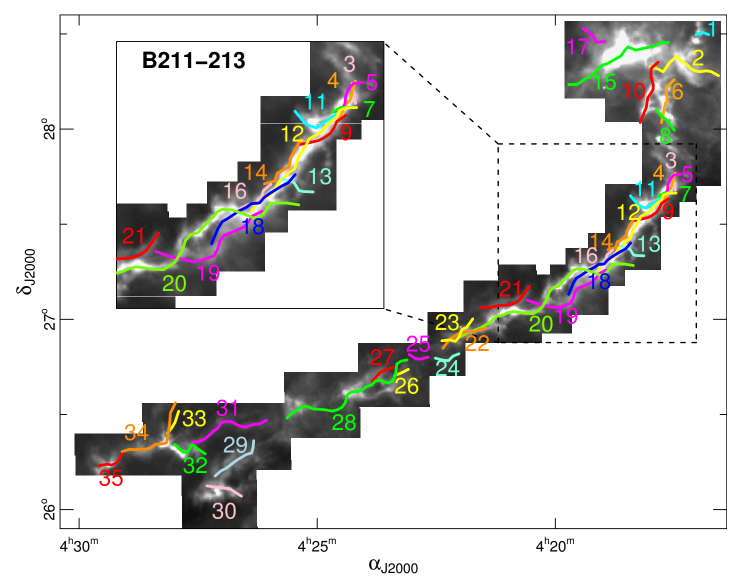

Smith et al. (2014, MNRAS, 445, 2900)

Summary

summary

- controversies / puzzles
  - column density PDFs: *do we really understand them?*
    —> ***more work needed, also on line PDFs***
  - molecular gas: *are we sure we see all H_2 gas?*
    —> ***we may be missing lots of H2 gas in clouds***
  - importance of dynamics: *what sets the IMF?*
    —> ***the IMF is easy to get, better look for other tracers***
  - filaments: *are they universal?*
    —> ***much more work needed including kinematic tracers***

NGC 3324 (Hubble, NASA/ESA)

thanks